Study on A Standing Wave Thermoacoustic Refrigerator Made of Readily Available Materials

Jinshah B S*, Ajith Krishnan R, Sandeep V S*****

*Department of Mechanical Engineering, Government Engineering College, Kozhikode, Kerala, India
**Department of Mechanical Engineering, Government Engineering College, Kozhikode, Kerala, India
***Department of Mechanical Engineering, Government Engineering College, Kozhikode, Kerala, India

Abstract- Use of CFC-contained systems has caused severe environmental hazards that have researchers looking for alternatives. Studies have shown that thermoacoustic technology is suited a candidate for conventional vapour compression cooling system in particular for special uses. In this research, theoretical, numerical and experimental studies were completed to identify optimum operating conditions for the design, fabrication, and operation of a thermoacoustic refrigerator. The system uses no refrigerant or compressor, and the only mechanical moving part is the loudspeaker connected to a signal generator that produces the acoustics. Here air at 1 atm is used as the working gas. The system fabricated with this grant is made of PVC and brass with a sinusoidal section to reduce power loss and can operate up to a maximum of 4 bar. The system can be taken apart if different stack geometry or material is to be studied.

Index Terms- Standing wave thermoacoustic refrigerator, stack, resonator column, acoustics, stirling cycle

I. INTRODUCTION

Thermoacoustics, as defined by Rott is a subject dealing generally with effects in acoustics in which heat conduction and entropy variations of a medium play a role. In this study the term thermo acoustics will be used in the limited sense of the generation of sound by heated surfaces and the process of heat transfer from one place to another by sound. In this section a brief review of the history of thermoacoustics is presented, along with a simple physical explanation of the effect, and some applications.

The development of thermoacoustic refrigeration is driven by the possibility that it may replace current refrigeration technology. Thermoacoustic refrigerators, which can be made with no moving parts, are mechanically simpler than traditional vapour compression refrigerators and do not require the use of harmful chemicals. Because of their simplicity, TARs should be much cheaper to produce and own than conventional technology. The parts are not inherently expensive, so even initial manufacturing costs should be low. Furthermore, mechanical simplicity leads to reliability as well as cheaper and less frequent maintenance. Until efficiency can be improved, operation costs may be higher; but with fewer moving parts, TARs require little to no maintenance and can be expected to have a lifetime much longer than ordinary refrigeration technology. Also, efficiency is likely to improve as thermoacoustic technology matures. Therefore, thermoacoustic refrigeration is likely to be more cost effective.

Besides reduced financial cost, environmental cost should be considered. Traditional vapour compression systems achieve their efficiencies through the use of specialized fluids that when released into the atmosphere (accidentally or otherwise) cause ozone depletion or otherwise harm the environment. Even most of the alternative fluids being developed cause harm in one way or another. For example, propane and butane won't destroy the ozone, but are highly flammable and pose a threat if a leak should occur. On the other hand, TARs easily accommodate the use of inert fluids, such as helium that cause no harm to the environment or people in the event of a leak. Also, normal operating pressures for TARs are about the same as for vapour compression systems, so thermoacoustic refrigeration is just as safe in that respect. Furthermore, TARs can be driven by TAEs in which case the input power can come from any source of heat, including waste heat from other processes. Then the combination TAE/TAR device has no negative impact on the environment and, in fact, can utilize energy sources that are otherwise wasted. Overall, thermoacoustic refrigeration is much more benign than conventional refrigeration methods in terms of environmental and personal safety.

One drawback, however, is a lack of efficiency in current TARs when compared to vapor compression. Traditional refrigeration techniques have the benefit of generations of research and application whereas thermoacoustic refrigeration is a new technology, so it is no wonder that vapour compression refrigerators are currently more efficient; however, there is reason to believe that thermoacoustic refrigeration will overtake vapour compression in the long run. The major reason is that a TAR can be driven with proportional control, but vapour compression schemes are binary (on/off). Although standing-wave TARs are currently less efficient than comparable conventional refrigerators, some of the difference can be made up when less than full power is required, which is most often the case. A normal refrigerator must switch off and on to maintain a given temperature; so the compressor is working its hardest whenever it is on, and the temperature actually oscillates around the desired value. In contrast, a refrigerator capable of proportional control, such as a TAR, can tune its power output to match the requirements of the load; so if the load increases a small amount, the refrigerator can slightly increase its power for a short time rather than running full tilt. This is especially advantageous in

applications where thermal shocks can cause damage, such as cooling electronics. As indicated above, it is absolutely possible—if not probable—that with expanded research efforts, thermoacoustic technology will become more efficient than vapour compression.

Due to its advantages in mechanical simplicity and environmental and personal safety, thermoacoustic refrigeration is becoming more important in the research community and may soon reach a point in its development when it can replace vapour compression as the primary technology used in refrigeration applications.

II. HISTORY

The generation of acoustic oscillations by heat have been observed and studied for over two centuries. Byron Higgins made the first observations and investigations of organ-pipe type oscillations, known as singing flames in 1777. At certain positions of a hydrogen flame inside a tube, open at both ends, acoustic oscillations were observed. Fig.(2.1) shows a configuration for producing Higgins oscillations. A survey of the phenomena related to Higgins oscillations was given by Putnam and Dennis.

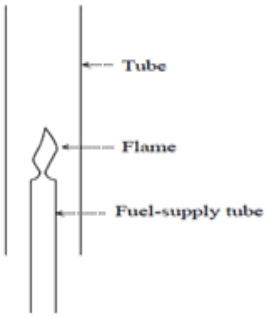

Figure 2.1: One form of the singing-flame apparatus. For certain position of
The flame inside the tube acoustic oscillations can be observed

In 1859, Rijke discovered that strong oscillations occurred when a heated wire screen was placed in the lower half of an open-ended pipe, as shown in Fig.(2.2). It was noticed that the convective air current through the pipe was necessary for the phenomenon to occur. Oscillations were strongest when the heated screen was located at one-fourth of the length of the pipe from the bottom end. Feldman gave a review of the literature on the Rijke tube [.Probably the research by Sondhauss, performed in 1860, approximates best what we define today as thermoacoustic oscillations. Sondhauss studied experimentally heat-generated sound, observed for centuries by the glass-blowers when blowing a hot bulb at the end of a cold narrow tube.

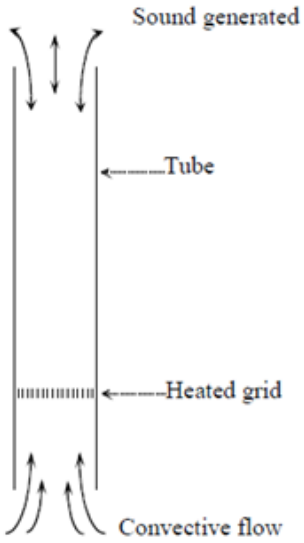

Figure 2.2: Rijke tube. The rijke acoustic oscillations can be observed best with the heated wire screen at one-fourth of the pipe from the bottom end

Fig.(2.3) a Sondhauss tube is shown; it is open on one end and terminated in a bulb on the other end. In Sondhauss observed that, if a steady gas flame (heat) was supplied to the closed bulb end, the air in the tube oscillated spontaneously and produced a clear sound which was characteristic of the tube length and the volume of the bulb. The sound frequency was measured and recorded for tubes having an inside diameter of 1 to 6mm, and having various bulb sizes and lengths. Hotter flames produced more intense sounds. Sondhauss gave no explanation for the observed oscillations. Feldman gave also a review of the literature on the Sondhauss tube . In

1962 Carter, during an experimental investigation of the feasibility of the Sondhauss tube to generate electricity, found that the insertion of a bundle of small glass tubes inside the Sondhauss tubes improved their performance. In 1887, Lord Rayleigh gave a qualitative explanation, in his classic work on sound for the Sondhauss oscillations. If heat be given to the air at the moment of greatest condensation or taken from it at the moment of greatest rarefaction, the vibration is encouraged. So Rayleigh knew that thermoacoustics was due to the interplay of heat injection and density variations.

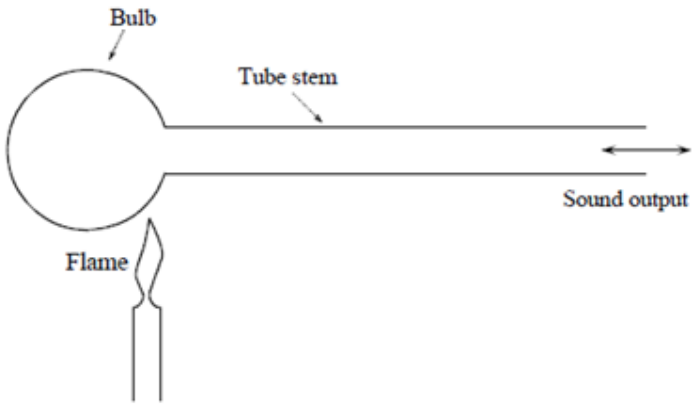

Figure 2.3: Soundhauss tube. When heat is supplied for example by means of a flame to the closed end, sound can be generated

Another form of Sondhauss oscillations, which occur in cryogenic storage vessels, are the so called .Taconis oscillations.. Taconis observed spontaneous oscillations when a hollow tube with the upper end closed was inserted in liquid helium. Taconis explanation of how the large temperature gradient along the tube caused the oscillations was essentially a restatement of the Rayleigh criterion. The Taconis oscillations have been studied experimentally by Yazaki et al. Although various aspects of what is now known as thermo acoustics have been of interest for centuries, the formal theoretical study of thermoacoustics started in 1949, when Kramers studied the Taconis oscillations. He generalized the Kirchhoff theory of the attenuation of sound waves at constant temperature to the case of attenuation in the presence of a temperature gradient. The results of Kramers theory were in disagreement with the experiment, because of some incorrect assumptions. In 1969, Rott continued the work of Kramers in a series of papers where a successful linear theory of thermoacoustics is given. Wheatley, Swift, and others have developed the connection between the acoustical part of thermo acoustics in a broader thermo dynamical perspective. Swift has reviewed much of this work. As can be understood from the above discussion, the history of heat-driven oscillations is rich and old. But the reverse thermodynamic process, of generating a temperature gradient by imposing acoustic oscillations, is a more recent phenomenon. Gifford and Longsworth demonstrated a heat-pumping process along the inner surface of a closed tube, where pressure pulses at low frequency were sustained . They called this cooling device a .Pulse tube, which is the precursor of the present orifice pulse-tube coolers. In 1975, cooling was also observed by Merkli and Thomann , at the velocity antinodes of a cylindrical cross-section acoustic tube in resonance. These two events formed the start of the work at Los Alamos National Laboratories (LANL) on thermoacoustic devices in the eighties, by Wheatley, Swift, and coworkers. The first acoustic heat pump (cooler), built at LANL, used a loudspeaker at one end of a closed tube to drive the acoustic resonance, and a stack of fiber glass plates positioned at the opposite end. The stack of plates was used to improve the thermoacoustic effect, as observed by Carter et al. With this arrangement, it was easy to produce a temperature difference over the stack, as a result of the heat transfer process from one end of the stack to the other. Since then, several experimental set-ups have been built.

III. BASIC PRINCIPLE OF THE THERMOACOUSTIC EFFECT

Acoustic waves consist not only of coupled pressure and displacement oscillations in a gas, but also of temperature oscillations as a response to the pressure variations. The interaction of these effects in gas close to a solid surface generates thermoacoustic oscillations. At the surface, heat can be extracted or supplied to the gas. The result of this interaction is that a sound wave is sustained in case of a large temperature gradient along the surface. While in the reverse case acoustic work is absorbed in order to transport heat, generating a temperature gradient. The mechanism of the thermoacoustic effect can best be visualized by considering a tube containing a gas, closed at one end and at the other an oscillating piston is moving forwards and backwards, compressing and expanding the gas in the tube, as shown in Fig.(3.1). In order to understand how the thermoacoustic cycle works, we follow a small volume of gas (parcel), as indicated by the small square in Fig(3.1), as it moves alongside the wall of the tube.

The motion of the piston is sinusoidal but for simplicity and clarity we consider a step by step cycle: (rapid motion-wait-rapid motion-wait-etc). This is indicated in Fig.(3.1) by the steps $[1-2-3-4-1-$ etc$]$.This cycle forms the thermodynamic cycle of the thermoacoustic effect. It consists of two reversible adiabatic steps 1 and 3 and two isobaric heat transfer steps 2 and 4, like in the Brayton cycle. The heat-pump process (refrigeration) occurs when the temperature gradient on the wall is zero or small, Fig.(3.1a). At the beginning of the cycle (step 1), the piston moves to the right in the direction of the closed end, compresses the parcel of gas which warms up. At this time, the parcel of gas is warmer than the local wall temperature, and heat flows irreversibly from the parcel to the wall (2). In step 3 the piston moves back, the parcel expands and cools. The parcel of gas is now colder than the local wall position,

and heat transfer from the wall to the parcel takes place (4). At this moment, the parcel of gas is at the initial position, and the cycle starts again.

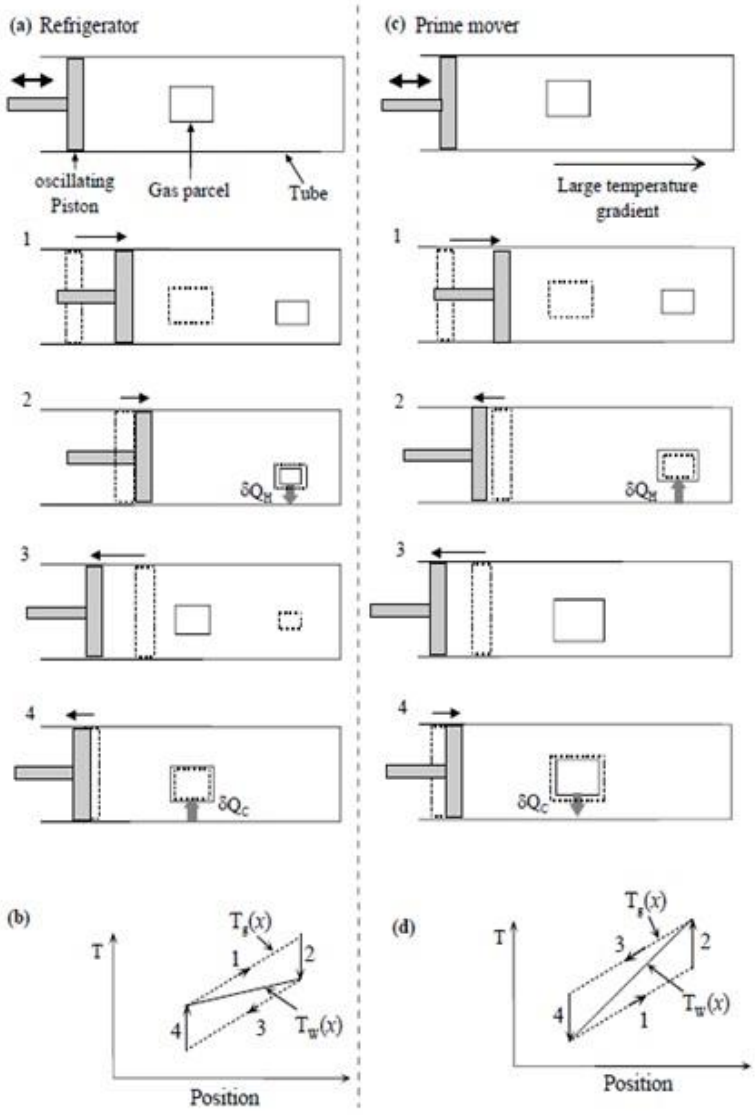

Figure 3.1: A typical gas parcel executing the four steps (1-4) of the cycle in a thermoacoustic refrigerator (left side)and prime mover (right side), assuming an inviscid gas and square wave acoustic motion and pressure. In each step, the dashed and solid squares are vertical triangles show the initial and final states of the parcel and piston, respectively. (b) gas temperature $T_g(x)$, and wall temperature $T_w(x)$versus position of the refrigerator. (d)Gas temperature $T_g(x)$, and Wall temperature $T_w(x)$ versus position for the prime mover.

As a result a small amount of heat is transported by the parcel of gas from the left to the right. After many cycles, a temperature gradient builds up along the tube and the piston end cools down and the closed end warms up. This process takes place as long as the temperature gradient in the gas, as a consequence of compression, is higher than the temperature gradient along the wall (and vise versa for the expansion). The work used to compress the gas in step 1, is returned in step 3, so that net no work is consumed in these two steps. During the heat transfer, step (2), the parcel of gas will contract and the piston has to move a little to the right to keep the pressure throughout the gas constant. In step (4), the piston has to move to the left.

A schematic pV-diagram for the refrigeration cycle, where V is the volume in front of the piston, is shown in Fig (3.2a).

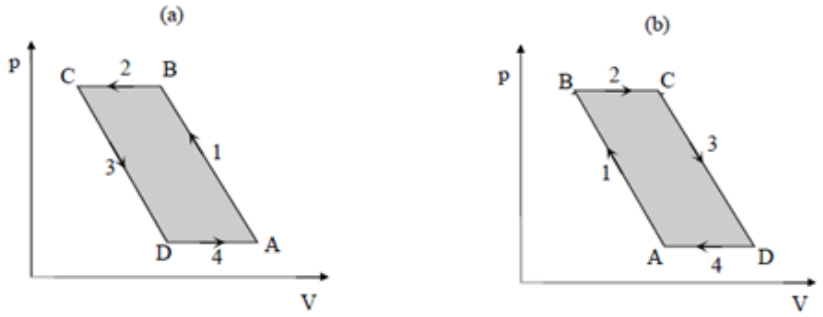

Figure 3.2: Schematic pV-diagram for the thermoacoustic cycle (Fig. (1.4)). a) Refrigerator; the area ABCD represents the work used. b) Prime mover; the area ABCD represents the work produced

The area ABCD represents the work used during the cycle. Actually, the whole gas alongside the wall of the tube contributes to the heat pump process. In Fig.(3.1c), the heat generation of sound in the so-called prime mover, is illustrated. The prime-mover cycle also consists of two adiabatic (1, 3) and two isobaric heat-transfer steps (2, 4). The only difference with the heat-pump case is that now we apply a large temperature gradient ΔT along the tube, so that the directions of heat transfer in steps 2 and 4 are reversed. When the parcel of gas is compressed, it warms up, but is still colder that the local wall position. Heat then flows from the wall into the parcel which expands. As a consequence of this expansion of the gas the piston will be pushed to the left and work is generated. In step 4, after the expansion, the gas element is warmer than the wall and heat flows into the wall. The gas contracts and work is done by the piston. The net work produced in one cycle is given by the area ABCD in Fig. (3.2b). As a result, a standing wave can be sustained by a large temperature gradient along the wall of the tube. In summary, during the compression step 1, the parcel of gas is both displaced along the wall and compressed. Two temperatures are important: the temperature of the gas after adiabatic compression and the local temperature of the wall adjacent to the parcel. If the temperature of the gas is higher than that of the wall, heat flows from the gas to the wall (heat pump). If the temperature of the gas is lower, heat flow sows from wall to gas (prime mover). Both heat flow and power can thus be reversed and the heat transfer process can be switched between the two modes by changing the temperature gradient along the wall. A small temperature gradient is the condition for heat pump; a high gradient is the condition for a prime mover. The gradient that separates the two regimes is called the critical temperature gradient. For this gradient, the temperature change along the wall matches the temperature change due to adiabatic compression, and no heat flows between the gas and the wall. The critical temperature gradient will be summarized in the next section. In the heat-pump regime work is absorbed to transfer heat from lower temperature to higher temperature. In this case, an acoustic wave has to be sustained in the tube to drive the process. In the prime mover mode the gas expands at high pressure (heat absorption), and contracts at low pressure (heat release), so that work is produced. In this case, the large temperature gradient sustains the acoustic oscillations. All periodic heat engines and refrigerators need some time phasing to operate properly. Conventional systems use pistons to compress and displace the gas in a given sequence. In thermoacoustic devices, this time phasing is ensured by the presence of the two thermodynamic media: gas and a solid surface, so that the irreversible heat transfer in steps 2 and 4 introduces the necessary time lag between temperature and motion. The compression and displacement are determined by the acoustic wave instead of pistons. At this stage, it is important to note that not all the gas in the tube is equally effective to the thermoacoustic effect. The elements of gas far away from the wall have no thermal contact, and are simply compressed and expanded adiabatically and reversibly by the sound wave. Elements that are too close to the wall have a good thermal contact, and are simply compressed and expanded isothermally. However elements at about a distance of a thermal penetration depth δk from the wall, have sufficient thermal contact to exchange some heat with the wall and produce a time delay between motion and heat transfer which is necessary for the heat pump process. The quantity δk is the distance across which heat can diffuse through the gas in a time $1/\pi f$, where f is the acoustic frequency.

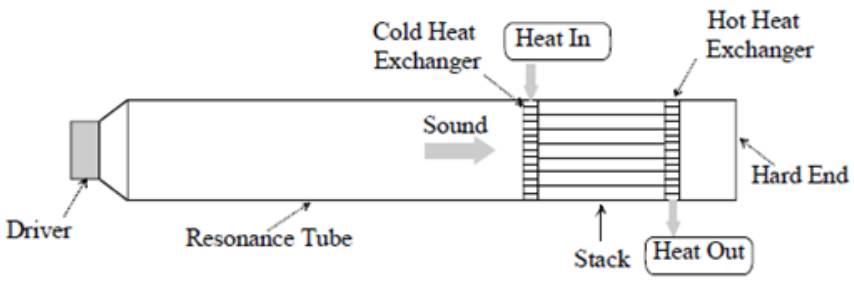

Figure 3.3: A simple illustration of a thermoacoustic refrigeration

As indicated in section II, Carter et al. realized that the performance of the thermoacoustic Sondhauss tube could be greatly improved by inclusion of a stack of small tubes. This has the effect of increasing the effective contact area between gas and solid over the cross-section of the tube, so that the whole gas contributes to the process. The appropriate use of stacks and their position in acoustically resonant tube scan produce powerful refrigerators (heat pump) and heat engines. We have to note here that even though the system uses a standing wave to displace, compress and expand the gas in the stack, a small travelling acoustic wave component is necessary to maintain the standing-wave resonance against the power absorption in the system. Systems using only traveling waves, which can be made more efficient, are also possible.

IV. APPLICATIONS

In previous section, the essentials of thermoacoustics were explained. Under favorable conditions, powerful or small size thermoacoustic devices can be built to operate as prime-movers or heat-pumps. Since the development of the first practical thermoacoustic apparatus in the early eighties at LANL, thermoacoustic technology has received an increasing attention as a new research area in heat engines and heat pumps. Since then, many thermoacoustic systems have been built, mostly at LANL, Naval Postgraduate School (NPS) in Monterey (California), and at Pennsylvania State University. Heat pumps and refrigerators use an acoustic driver (loudspeaker or prime mover)to pump heat from a cool source to a hot sink. A simple thermoacoustic refrigerator is shown in Fig.1.6. Such systems contain a loudspeaker, which drives an intense sound wave in a gas-filled acoustical resonator. A structure with channels, called the stack is appropriately placed in the tube. The stack is the heart of the refrigerator where cooling takes place. Two examples of refrigerators that were built and tested at NPS are: The Space Thermoacoustic Refrigerator (STAR), which was designed to produce up to 80K temperature difference over the stack, and to pump up to 4 watt of heat. The STAR was launched on the space shuttle Discovery in 1992. The second setup is the Shipboard Electronics Thermo Acoustic Cooler (SETAC) that was used to cool radar electronics on board of the warship USS Deyo in 1995. It was designed to provide 400watt of cooling power for a small temperature span, which is similar to a domestic refrigerator/freezer system. At Pennsylvania State University, a large chiller called TRITON is being developed to provide cooling for Navy ships. It is intended to produce a cooling power of about 10 kW which means that it can convert three tons of water at 00C to ice at the same temperature in one day. At LANL, a heat-driven thermoacoustic refrigerator known as the beer cooler was built, which uses a heat-driven prime mover instead of a loudspeaker to sound necessary to drive the refrigerator. A similar device, called a Thermoacoustic Driven Thermo Acoustic Refrigerator (TADTAR) was recently built at NPS. It has a cooling power of about 90 watt for a temperature span of 25 ^{0}C. Such a device has no moving parts at all. Also at NPS, a solar driven TADTAR has been built which has a cooling capacity of 2.5 watt for a temperature span of 17.7 ^{0}C

At LANL, much of the efforts focused primarily on large thermoacoustic engines, using heat to generate sound, which is used to generate electrical power or to drive coolers to liquefy natural gas. One example of such efforts is collaboration between LANL and an industrial partner to develop a cryogenic refrigeration technology called Thermo Acoustically Driven Orifice Pulse Tube refrigeration (TADOPTR). This technology has the unique capability of producing cryogenic temperatures (115 K) with no moving parts. It uses a pulse-tube refrigerator which is driven by a natural-gas-powered thermoacoustic prime mover. A machine with a cooling capacity of 2kW producing about 0.5 m3/day, has been developed. A second system, using a traveling wave prime mover, is now under construction. This has a higher efficiency, and a cooling capacity of about 140 kW. It is expected that it will burn 20 % of natural-gas to liquefy the other 80 % at a rate of about 50 m^3/day. At Tektronix, a TADOPTR was also built to provide cooling of electronic components. The prime mover, used in this cooler, provided 1 kW to the pulse-tube refrigerator with an efficiency of about 23% of Carnot. The prime mover was driven by an electric heater. Hence the system had no moving parts. The potential of applications of thermoacoustic devices is substantial, as can be understood from the foregoing examples. Prime movers can be used to generate electricity, or to drive refrigerators. Thermoacoustic heat pumps can be used to generate heating, air-conditioning or cooling of sensors, supercomputers, etc. Their advantage is that they can have one (loudspeaker) or no moving parts no tight tolerances, making them potentially reliable and low cost. Besides being reliable, they use only inert gases (no CFC.s) so they are environmentally friendly. On the other hand, standing-wave thermoacoustic devices have a relatively low efficiency. However, thermoacoustics still a young technology. Recently, the LANL team has designed a traveling-wave prime-mover which has efficiency much higher than the standing-wave counterpart. This engine is a Stirling version of the thermoacoustic prime-mover. It has a thermal efficiency of 30 % while typical internal combustion engines are 25 to 40% efficient. Thermoacoustic refrigerators can also be made using this principle, and reach efficiencies comparable to vapor compression systems. Swift gave an excellent review of the current status of the field of thermoacoustics in his introductory book .

V. BASIC THERMODYNAMIC AND ACOUSTIC CONCEPTS

This section presents the underlying thermodynamic and acoustic principles, and discusses the interplay of these effects in thermoacoustics. The section starts with a review of the thermodynamic efficiency of a heat engine and the coefficient of performance of a refrigerator and heat pump. Then, a description of the thermo dynamics of the gas oscillating in the channels of a stack will be introduced. Simple expressions for the heat flow and acoustic power used in the stack will be derived. After that, the acoustics of thermoacoustic devices will be illustrated, and the important concepts for the operation will be explained. Finally, some basic measurements with a simple thermoacoustic refrigerator will be used to clarify the discussed effects.

V.I. THERMODYNAMIC PERFORMANCE

In this section the thermal efficiency for prime movers and the coefficient of performance for refrigerators and heat pumps are introduced, using the first and second law of thermodynamics. From the thermodynamic point of view, prime movers are devices that, per cycle, use heat Q_H from a source at a high temperature T_H and reject waste heat to a source at a lower temperature T_C, to generate work W. On the other hand, refrigerators and heat pumps are devices that use work W to remove heat Q_C at a temperature T_C and reject Q_H at a higher temperature T_H. These devices are illustrated in Fig.(5.1).

The energy flows into and out of thermodynamic systems are controlled by the first and second law of thermodynamics. The first law of thermodynamics is a statement of the energy conservation: the rate of increase or decrease of the internal energy U of a thermodynamic system of volume V equals the algebraic sum of the heat flows, and enthalpy flows into the system, minus the work done by the system on the surroundings;

$$\dot{U} = \sum \dot{Q} + \sum \dot{n} H_m - p\dot{V} + P \qquad (5.1)$$

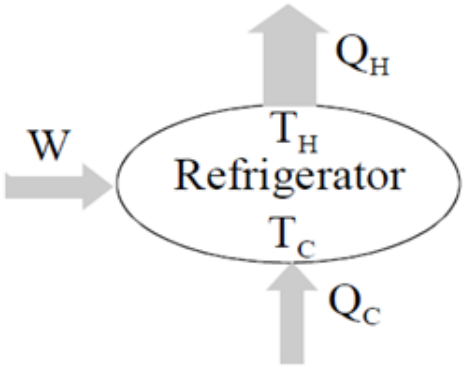

Figure 5.1: Representation of a refrigeration of a refrigerator while exchanging per cycle heat and work with the surroundings. The directions of heat and work exchanged between the refrigerator and its environment are shown by the shaded arrows. In a prime mover the directions of the arrows are reversed.

where $\dot{n}$ is the molar flow rate of matter flowing into the system, H_m is the molar enthalpy, and P represents other forms of work done on the system. The summations are over the various sources of heat and mass in contact with the system; transfers into the system are positive and those out of the system are negative. The second law of thermodynamics limits the interchange of heat and work in thermodynamic systems. This law states that the rate of change of entropy of a thermodynamic system is equal to the algebraic sum of the entropy change due to the heat flows, due to the mass flow, and due to the irreversible entropy production in the system [1]

$$\dot{S} = \sum \frac{\dot{Q}}{T} + \sum \dot{n} S_m + S_i \qquad (5.2)$$

where the summation is over the various sources with the same sign convention as stated above. The heat flow, $\dot{Q}$, into or out of the system, takes place at the temper-ature T. In addition the second law of thermodynamics requires that

$$\dot{S}_i \geq 0 \qquad (5.3)$$

In the following the first and second law of thermodynamics, Eqs.(5.1)-(5.3), will be used to define the performance for refrigerators, heat pumps and prime movers.

V.I.I. REFRIGERATORS AND HEAT PUMPS

The duty of a refrigerator or heat pump is to remove a heat quantity Q_c at a low temperature T_C and to supply a heat quantity Q_H to the surroundings at a high temperature T_H. To accomplish these processes a net work input, W, is required. This process is illustrated in Fig.(5.1). Refrigerators and heat pumps have different goals. The goal of a refrigerator is to maintain the temperature of a given space below that of the surroundings. While the goal of a heat pump is to maintain the temperature of a given space above that of the surroundings. Since refrigeration and heat pump systems have different goals, their performance parameters, called coefficient of performance (COP) are defined differently. By considering the refrigerator illustrated in Fig.(5.1) and using the fact that there is no mass flow into or out of the system, the first and second law, Eqs.(5.1) and (5.2),take the simple form

$$\dot{U} = \dot{Q}_C - \dot{Q}_H + \dot{W} \qquad (2.4)$$

And

$$\dot{S} = \frac{\dot{Q}_C}{T_C} - \frac{\dot{Q}_H}{T_H} + \dot{S}_i \qquad (5.5)$$

Where U and S are the internal energy and entropy of the system, respectively; S_i is the irreversible entropy production in the system. The integration over one cycle of Eqs.(5.4) and (5.5), and the use of the fact that U and S are functions of state which do not change over one cycle, yields

$$Q_H = \dot{Q}_C + W \tag{5.6}$$

And

$$\frac{Q_H}{T_H} = \frac{Q_C}{T_C} + \dot{S}_i \tag{5.7}$$

V.I.I(A). REFRIGERATOR

In the case of a refrigerator we are interested in the heat removed Q_C at T_C, and the net work used to accomplish this effect, W. The COP_{ref} is given by the ratio of the quantities, thus

$$COP_{ref} = \frac{Q_C}{W} \tag{5.8}$$

Substituting Eq.(5.6) into Eq.(5.8) yields

$$COP_{ref} = \frac{Q_C}{Q_H - Q_C} \tag{5.9}$$

Since $Si \geq 0$, Eq.(5.7) gives

$$\frac{Q_C}{T_C} \leq \frac{Q_H}{T_H} \tag{5.10}$$

Combining Eq.(5.9) with Eq.(5.10) gives

$$COP_{ref} \leq \frac{T_C}{T_H - T_C} \tag{5.11}$$

$$COP_C = \frac{T_C}{T_H - T_C} \tag{5.12}$$

The quantity is called the Carnot coefficient of performance which is the maximal performance for all refrigerators. This COP can be made larger than one if $T_C > T_H/2$. The coefficient of performance relative to Carnot's coefficient of performance is defined as

$$COP_R = \frac{COP}{COP_C} \tag{5.13}$$

V.I.I(B). HEAT PUMP

The performance of heat pumps is defined as the ratio of the desired heat, Q_H, to the net work needed W. For a heat pump we are interested in the heat Q_H supplied to a given space. Thus the coefficient of performance, COP_{hp}, is

$$COP_{hp} = \frac{Q_H}{W} \tag{5.14}$$

In combination with Eq.(5.6), this gives

$$COP_{hp} = \frac{Q_H}{Q_H - Q_C} \tag{5.15}$$

This expression shows that the value of the COP_{hp} is always larger than unity. Combining Eq.(5.15) and Eq.(5.10) leads to the expression

$$COP_{hp} \leq \frac{T_H}{T_H - T_C} \tag{5.16}$$

The temperature expression on the right is called the Carnot COP_{hp} which is the maximum performance for all heat pumps. The coefficients of performance COP_{ref} and COP_{hp} are defined as ratios of the desired heat transfer output to work input needed to accomplish that transfer. Based on the definitions given above, it is desirable thermodynamically that these coefficients have values that are as large as possible. As can be seen from Eqs. (5.11), (5.16), the second law of thermodynamics imposes limits on the performance, because of irreversibility in the system.

V.I.II. EFFICIENCY OF THE PRIME MOVER

Since the prime mover uses heat Q_H to produce work W the directions of heat and work flows in Fig.(5.1) are reversed. The performance η of a prime mover is defined as the ratio of the produced work (output) and the heat used to produced that work(input), thus

$$\eta = \frac{W}{Q_H} \tag{5.17}$$

By use of Eq.(5.6), we have

$$\eta = \frac{Q_H - Q_C}{Q_H} \tag{5.18}$$

This expression shows that the efficiency of a prime mover is less than one. Since Q_H is entering the prime mover and Q_C is flowing out of it, Eq.(5.10) becomes

$$\frac{Q_C}{T_C} \geq \frac{Q_H}{T_H} \tag{5.19}$$

In a similar way as described above, we can derive the well-known relation

$$\eta \leq 1 - \frac{T_C}{T_H} \tag{5.20}$$

The temperature expression on the right is called the Carnot efficiency, which is the maximal performance for all prime movers.

V.II. THERMODYNAMIC APPROACH TO THERMOACOUSTICS

A simplified picture of the thermoacoustic effect will be given, using only thermo-dynamics and acoustics to explain how a temperature gradient and hence cooling develops across a stack. The discussion in this section is concerned with the derivation of approximate expressions for the critical temperature gradient and the heat and work flows in thermoacoustic devices. The papers of Wheatley and Swift form the basis for the discussion in this section. Most of the matter and illustrations discussed in the previous section will be repeated here for ease of discussion and derivation of thermoacoustic quantities.

As discussed in the preceding section, thermoacoustic devices consist mainly of an acoustic resonator filled with a gas. In the resonator, a stack consisting of a number of parallel plates, and two heat exchangers, are appropriately installed (Fig.(5.2a)).The stack is the element in which the heat-pumping process takes place. The heat exchangers are necessary to exchange heat with the surroundings, at the cold and hot sides of the stack, as shown in Fig.(5.2a). A loudspeaker sustains an acoustic standing wave in the acoustic resonator. As an approximation, we neglect the viscosity of the gas and the longitudinal thermal conductivity. In response to the acoustic wave, the gas oscillates in the stack channels and is compressed and expanded.

We begin by discussing the thermodynamics of a small parcel of gas oscillating along a stack plate, being compressed and expanded by the sound wave. An average longitudinal temperature gradient ΔT_m along the stack is supposed to exist. Addition-ally, we suppose that the pressure antinodes is to the right of the plate and a node to the left (Fig.(5.2b)). For simplicity, the following treatment will assume an in viscid ideal gas of vanishing Prandtl number The four steps of the thermoacoustic cycle are illustrated separately in Fig.(5.3).

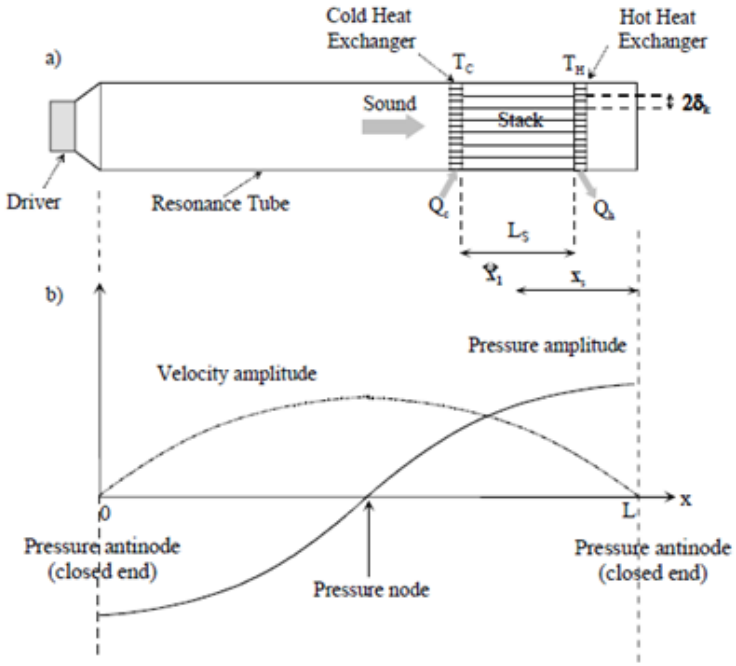

Figure 5.2: Model of a thermoacoustic refrigerator. (a) An acoustically resonant tube containing a gas, a stack of parallel plates and two heat exchangers. An acoustic driver is attached to one end of the tube and the other end is closed. Some length scales are also shown: the gas excursion in the stack x_1, the length of the stack L_s, the position of the stack from the closed end x_s and spacing in the stack $2\delta_k$. b) Illustration of the standing wave pressure and velocity in the resonator.

We suppose that, in the start of the cycle, the temperature, pressure, and volume of the parcel are $T_m - x_1\Delta T_m$, $p_m - p_1$, and V. In step 1, the parcel of gas moves a distance $2x_1$, is compressed and increases in temperature by an amount $2T_1$. The adiabatic Pressure change p_1 and temperature change T_1 are related by the thermodynamic relationship,

$$T.ds = c_p.dT + \frac{T}{\rho^2}\left(\frac{\partial\rho}{\partial T}\right)_p.dp = 0 \qquad (5.21)$$

where s is the specific entropy, ρ is the density, c_p is the isobaric specific heat per unit mass, T is the absolute temperature, and p is the pressure. This expression can be rewritten as;

$$T_1 = \left(\frac{\beta T}{\rho . c_p}\right)_m p_1 \quad (5.22)$$

where

$$\beta = -\frac{1}{\rho}\left(\frac{\partial \rho}{\partial T}\right)_p \quad (5.23)$$

The subscript m indicates that we are concerned with the mean value of the quantities between brackets. The parameter β is the isobaric volumetric expansion coefficient. Considering an ideal gas ($\beta T_m = 1$) and using the ideal gas law, the expression (5.22) becomes

$$\frac{T_1}{T_m} = \left(\frac{\gamma - 1}{\gamma}\right)\frac{p_1}{p_m} \quad (5.24)$$

where γ is the ratio of isobaric to isochoric specific heats.

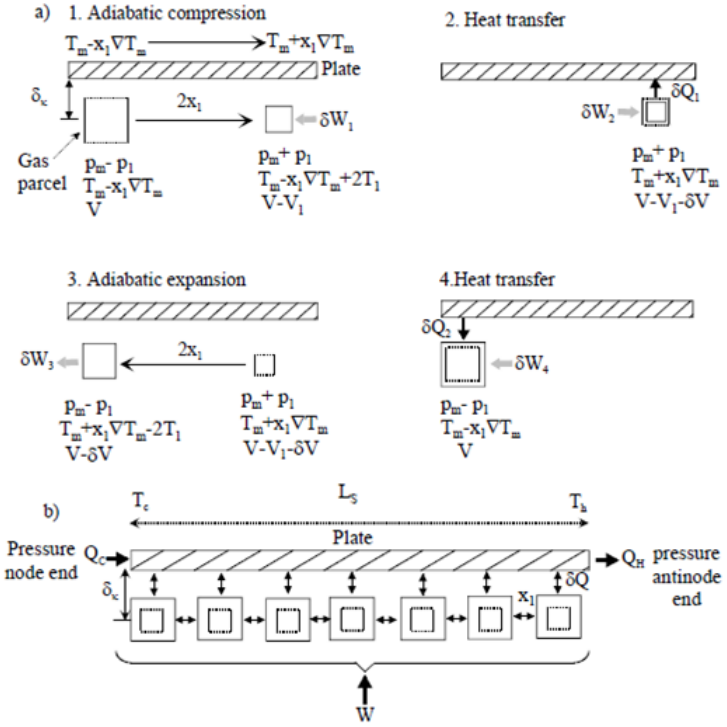

Figure 5.3: a) Typical gas parcel in a thermoacoustic refrigerator passing through a four-step cycle with two adiabats (step 1 and 2) and two constant-pressure heat transfer steps (2 & 4). B) an amount of heat is shuttled along the stack plate from one parcel of gas to another, as a result Q is transported from the left end of the plate to the right end, using work W. the heat increases in the stack from Q_c to Q_h.

After the displacement and compression in step 1, the temperature, pressure and volume becomes $T_m - x_1\Delta T_m + 2T_1$, $p_m + p_1$, and $V - V_1$. At this time, the temperature difference between the plate and the parcel of gas is

$$\delta T = 2.T_1 - 2.x_1\Delta T_m \quad (5.25)$$

where $2x_1\Delta T_m$ is the temperature change along the plate. In step 2, for positive δT, heat δQ flows from the parcel of gas to the plate at constant pressure. The heat that flows out of the parcel is given by

$$\delta Q \approx mc_p\delta T \quad (5.26)$$

where m is the mass of the parcel of gas.

In Fig.(5.4), a schematic pV -diagram of the cycle is shown. The work used in the cycle is equal to the area ABCD, and given by

$$\delta W = \int_{ABCD} p.dV \quad (5.27)$$

The used acoustic power in each step is shown in Fig.(5.4). Using the acoustic approximation, p_1, p_m, and the Poisson's law for the two adiabatic steps, the result after calculation is

$$\delta W \approx -2p_1\delta V \quad (5.28)$$

The volume δV is related to δT by Eq.(5.23),

$$\delta V = (\beta V)_m\delta T \quad (5.29)$$

Insertion into Eq.(5.28) yields

$$\delta W = -2p_1(\beta V)_m\delta T \quad (5.30)$$

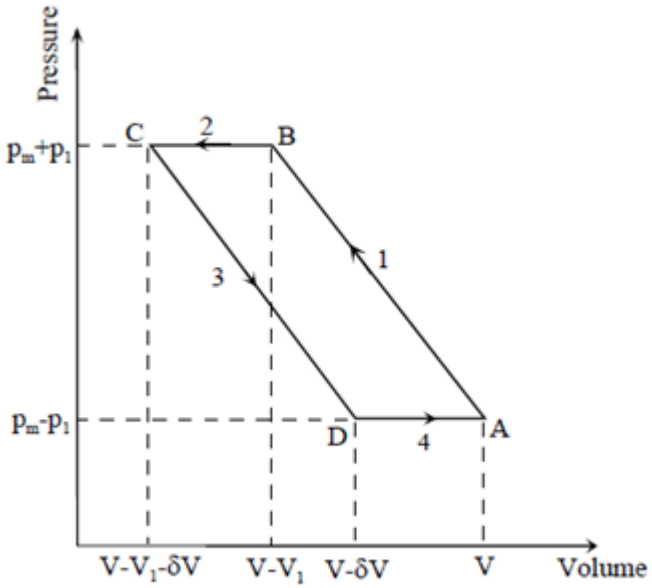

Figure 5.4: Schematic pV-diagram of the thermoacoustic cycle of Fig.(2.3). the four steps of the thermoacoustic cycle are illustrated: adiabatic compression (1), isobaric heat transfer (2), adiabatic expansion (3) and isobaric heat transfer (4). The area ABCD is the work used in the cycle which is also egal to the different steps.

In step 3, the parcel of gas moves back to its initial position, expands and cools. At this time, the parcel of gas is colder than the local stack surface, and heat δQ flows into the parcel (step 4).In case δT is negative, heat flows into the parcel which expands and does work δW on its surroundings (prime mover). The sign of the temperature difference δT(and hence magnitude of ΔT_m) determines, after displacement and compression, the direction of the heat flow, into or out of the parcel of gas. Therefore, the refrigerator mode and prime mover mode can be distinguished by the sign of δT. If the temperature change $2x_1\Delta T_m$ in the plate just matches the adiabatic temperature change $2T_1$, then the temperature gradient in the stack is named the critical temperature and is given by

$$(\Delta T)_{crit} = \frac{T_1}{x_1} \tag{5.31}$$

Using Eq.(5.22) and $x_1 = u_1/\omega$, where u=1 is the gas particles velocity amplitude and ω the angular frequency, we obtain

$$(\Delta T)_{crit} = \frac{p_1\omega}{\rho_m c_p u_1} \tag{5.32}$$

The two modes of operation are characterized in terms of the ratio of the temperature gradient along the stack and the critical temperature gradient

$$\Gamma = \frac{\Delta T_m}{(\Delta T)_{crit}} \tag{5.33}$$

Employing Eqs.(5.33), (5.22) and assuming an ideal gas ($\beta_T = 1$) we can rewrite Eqs.(5.26) and (5.30), as

$$\delta Q \approx -2Vp_1(\Gamma - 1) \tag{5.34}$$

And

$$\delta W \approx 4\left(\frac{p_1^2 V\beta}{\rho c_p}\right)_m (\Gamma - 1) \tag{5.35}$$

respectively. As can be seen from Fig.(5.5), if we suppose that Π is the perimeter of the plate in the direction normal to the axis of the resonator, L_s is the length of the plate parallel to the resonator axis (wave direction), and since only the layer of gas at a distance δk from the plate contributes to the thermoacoustic heat transport, the effective volume rate of flow of the gas is $\Pi\delta_k u_1$. Here u_1 is the amplitude of the speed of motion of the gas, caused by the sound wave.

The thermoacoustic heat flow rate along the plate from T_C to T_H (refrigerator mode) is obtained by replacing V in Eq.(5.34) by the effective volume flow $\Pi\delta_k u_1$, i.e.

$$\dot{Q} \approx -2\Pi\delta_k p_1 u_1(\Gamma - 1) \tag{5.36}$$

The total volume of gas that is thermodynamically active along the plate is $\Pi\delta_k L_s$, so that the total work used to transport heat is given by

$$W \approx \frac{4\Pi\delta_k L_s p_1^2\beta}{\rho_m c_p}(\Gamma - 1) \tag{5.37}$$

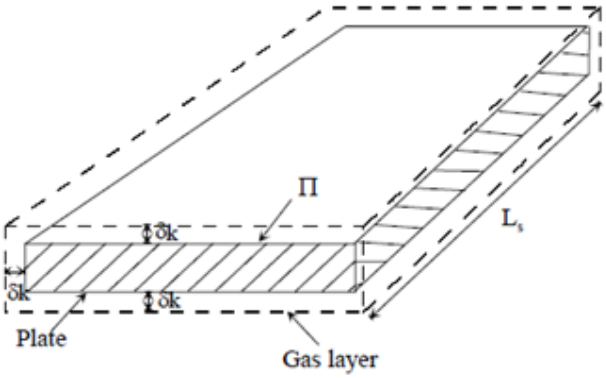

Figure 5.5: A single stack plate at length L_s and perimeter Π. The gas layer at a distance δ_k from the plate is shown by dashed line. The gas area is equal to $\Pi\delta_k$ and the total volume of gas in contact with the plate is $\Pi\delta_k L_s$.

The power needed to pump the heat is the work per cycle times the frequency ω, so that

$$\dot{W} \approx \omega \frac{4\Pi\delta_k L_s p_1^2 \beta}{\rho_m c_p}(\Gamma - 1) \qquad (5.38)$$

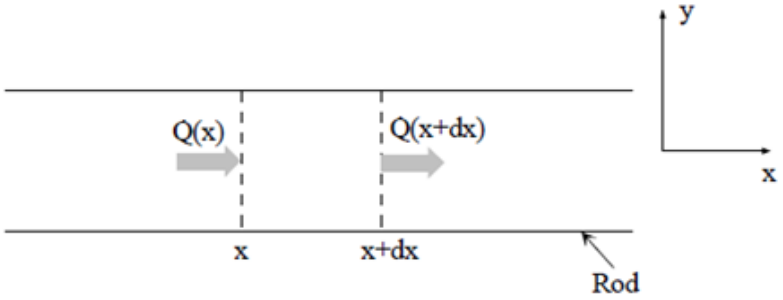

Figure 5.6: illustration used in the derivation of the heat conduction equation

When use is made of the definition of the speed of sound and the ideal gas law,

$$a^2 = \gamma \frac{p_m}{\rho_m} = T_m c_p(\gamma - 1) \qquad (5.39)$$

where $\gamma - 1$ is the work parameter of the gas, we can rewrite Eq.(5.38) as

$$\dot{W} \approx \omega \frac{4\Pi\delta_k L_s(\gamma-1)p_1^2}{\rho_m a^2}(\Gamma - 1) \qquad (5.40)$$

A quantitative evaluation of Q and W for sinusoidal p_1 and $u_1$would give the same results except that each expression has a numerical prefatory of 14 . The total heat flow and absorbed acoustic power in the stack can be obtained by using the total perimeter of the plates Π_{tot} instead of the perimeter of one plate Π.

Expressions (5.36) and (5.38) change sign as Γ passes through unity. Three cases can be distinguished: Γ = 1, there is no heat flow and no power is needed; When Γ < 1, the heat is transported against the temperature gradient so that external power is needed, and the device operates as a refrigerator; Γ > 1, due to the large temperature gradient, work is produced, and the device operates as a prime mover. Therefore, the device can operate as a refrigerator as long as the temperature gradient over the plate (stack) is smaller than the critical temperature gradient (Eq.(5.31)).But we can impose a large temperature gradient over the plate so that the device Operates as a prime mover (Γ > 1).

As stated previously, the thermoacoustic effect occurs within the thermal penetration depth δk, which is roughly the distance over which heat can diffuse through the gas in a time 1/πf, where f denotes the frequency of the acoustic wave. In Fig.(5.6),the heat conduction in one dimension through a rod of cross-section A is illustrated. Considering the energy balance for a small element dx of the rod, we suppose that heat is the only form of energy that enters or leaves the element dx, at x and x+dx, and that no energy is generated inside the element. Energy conservation yields

$$\rho_s A \frac{\delta u}{\delta t} = -\frac{\delta \dot{Q}}{\delta x} \qquad (5.41)$$

The heat flow is given by the Fourier's law of heat conduction

$$\dot{Q} = -K_s A \frac{dT}{dX} \quad (5.42)$$

Where K_s is the thermal conductivity of the material. Substituting Eq.(5.42) and the thermodynamic expression $du = c_s dT$ for the internal energy of solid-state material into Eq.(5.41) yields

$$\frac{\rho_s c_s}{K_s}\frac{\partial T}{\partial t} = \frac{\partial^2 T}{\partial x^2} \quad (5.43)$$

where c_s and ρ_s are the isobaric specific heat and density of the material, respectively. If we substitute the characteristic dimensions $\delta_s = x/x_0$ and $t_0 = \omega t$ into Eq.(5.43) we

Get

$$\frac{\rho_s c_s \omega}{K_s}\frac{\partial T}{\partial t'} = \frac{1}{\delta_s^{(2)}}\frac{\partial^2 T}{\partial x'^2} \quad (5.44)$$

so that

$$\delta_s^{(2)} = \frac{K_s}{\rho_s c_s \omega} \quad (5.45)$$

and hence

$$\delta_s = \sqrt{\frac{K_s}{\omega}} \quad (5.46)$$

where κ_s is the thermal diffusivity, $\kappa_s = K_s/\rho_s c_s$. A similar procedure can be used to derive an analogous expression for the thermal penetration in a gas. Closely related to the thermal penetration depth is the viscous penetration depth in a gas $\delta\nu$. It is roughly the distance over which momentum can diffuse in a time $1/\pi f$ and it is given by

$$\delta_\nu = \sqrt{\frac{2\upsilon}{\omega}} \quad (5.47)$$

where the kinematic viscosity ν is given by

$$\upsilon = \frac{\eta}{\rho} \quad (5.48)$$

here η is the dynamic viscosity of the gas. An important parameter for the performance of thermoacoustic devices is the Prandtl number σ, which is a dimensionless parameter describing the ratio of viscous to thermal effects

$$\sigma = \frac{\eta c_p}{K} = \left(\frac{\delta_\upsilon}{\delta_k}\right)^2 \quad (5.49)$$

For most gases (air, inert gases) but not gas mixtures, σ is nearly 2/3 , so that for these gases thermal and viscous penetration depths are quite comparable. The effect of viscosity on the heat flow and acoustic power will be discussed in the next section.

V.III. ACOUSTIC CONCEPTS

In this section, some acoustic concepts which are important for proper operation of thermoacoustic devices will be described. The discussion will be limited to standing wave thermoacoustic devices, which are more related to the subject of this research.A simple illustration of a thermoacoustic refrigerator is shown in Fig.(5.2). It consists of an acoustic resonator (tube) of length L (along x) and radius r. The resonator is filled with a gas and closed at one end. An acoustic driver, attached to the other end, sustains an acoustic standing wave in the gas, at the fundamental resonance frequency of the resonator. A stack of parallel plates and two heat exchangers are appropriately installed in the resonator.The first condition for the proper operation of thermoacoustic refrigerators is that the driver sustains an acoustic wave. This means that the driver compensates for the energy absorbed in the system. Hence, a small travelling wave component is superimposed on a standing wave; we have to note that in a pure standing wave there is no energy transport.

To illustrate the acoustics, we consider for simplicity that the stack and the heat exchangers have no effect on the acoustic field in the tube. The driver excites a wave along the x direction. The combination of a plane traveling wave to the right and there affected wave at the closed end of the tube generates a sinusoidal standing wave. The acoustic pressure in the tube is given by

$$p(x,t) = p_1(x)\sin\omega t$$
$$p_1(x) = p_0 \cos kx \quad (5.50)$$

Where p_0 is the pressure amplitude at the pressure antinodes of the standing wave, ω is the angular frequency of the wave, k is the wave number. By integration of Newton's second law (acoustic approximation), $\rho\,\partial u/\partial t = -\partial p/\partial x$, thegas particle velocity is

$$u(x,t) = u_1(x)\cos\omega t$$
$$u_1(x) = \frac{p_0}{\rho_m a}\sin kx \quad (5.51)$$

where

$$k = \frac{\omega}{a} \quad (5.52)$$

From the fact that sin kx is zero where cos kx is maximum and vice versa, it follows that pressure antinodes are always velocity nodes and vice versa; the pressure and velocity are spatially 90 degrees out-of-phase.

The frequency of the acoustic standing wave is determined by the type of gas, the length L of the resonator and the boundary conditions. A quarter-wavelength resonator is suitable, for many reasons as will be illustrated in upcoming section. But a half-wavelength resonator can also be used. This depends on how the standing wave Þts in the tube. A half-wavelength resonator has two closed ends, so that the velocity is zero at the ends and the pressure is maximal (antinodes). The resonance modes are given by the condition that the longitudinal velocity vanishes at the ends of the resonator is used.

$$\sin kL = 0 \quad (5.53)$$

Hence,

$$\lambda = \frac{2L}{n}(n = 1,2,3,4, \dots \dots \dots) \quad (5.54)$$

Where

$$k = \frac{2\pi}{\lambda} \quad (5.55)$$

In this case we see that the first (fundamental) mode which is usually used in thermoacoustic devices, corresponds to L = λ/2, ergo the name half-wavelength resonator. For a quarter-wavelength resonator, one end is open and the other end is closed. This requires a pressure node at the open end, hence

$$\cos kl = 0 \quad (5.56)$$

So that

$$\lambda = \frac{4L}{2n-1}(n = 1,2,3, \dots \dots \dots) \quad (5.57)$$

The fundamental mode corresponds to L = λ/4, ergo the name quarter-wave resonator. The refrigerator shown in Fig.(5.2), is assumed to be a half-wavelength device. Thus, in the resonance tube, we obtain the pressure and velocity distributions indicated in Fig.(5.2b).

V.IV. BASIC OPERATION CONCEPTS

In the previous sections some basic thermodynamic and acoustic concepts have been introduced. In this section, we will illustrate the effect of the position of the stack in the standing-wave field on the behavior of the thermoacoustic devices .In Fig.(5.2), some important length scales are also shown: the longitudinal lengths, wavelength λ = 2L, gas excursion x_1, stack length L_S, and the mean stack position from the pressure antinode x_S, and the transversal length: spacing in the stack 2δk.For audio frequencies, we have typically for thermoacoustic devices:

$$\frac{1}{k} = \frac{\lambda}{2\pi} \gg x_s \geq L_s > x_1 \quad (5.58)$$

Since the sinusoidal displacement x_1 of gas parcels is smaller than the length of the plate L_s, there are many adjacent gas parcels, each confined in its cyclic motion to a short region of length $2x_1$, and each reaching the extreme position as that occupied by an adjacent parcel half an acoustic cycle earlier (Fig.(5.3b)). During the first half of the acoustic cycle, the individual parcels move a distance x_1 toward the pressure antinodes and deposit an amount of heat δQ at that position on the plate. During the second half of the cycle, each parcel moves back to its initial position, and picks up the same amount of heat, that was deposited a half cycle earlier by an adjacent parcel of gas. The net result, is that an amount of heat is passed along the plate from one parcel of gas to the next in the direction of the pressure antinode as shown in Fig.(5.3b).

Finally, we note that, although the adiabatic temperature T_1 of a given parcel maybe small, the temperature difference ΔT_m over the stack can be large, as the .number of parcels., L_s/x_1, can be large (Fig.(5.3b)). As from Eq.(5.33)

we find

$$\Gamma = \frac{\Delta T_m}{(\Delta T)_{\text{crit}}} = \frac{\frac{\nabla T_m}{L_S}}{\frac{T_1}{x_1}} \quad (5.59)$$

We find

$$\nabla T_m = \frac{L_S}{x_1}\frac{T_1}{\Gamma} \quad (5.60)$$

Since Γ < 1, and L_s À x_1, we see that ΔT_m can be made much larger than T_1.

V.IV.I. TEMPERATURE GRADIENT

The gas harmonic excursion, x_1 is given by

$$x_1 = \frac{u_1}{\omega} \quad (5.61)$$

Hence, close to a pressure antinode (velocity node) the excursion of a typical parcel of gas is small. At the same time the parcel experiences large changes in pressure and a large adiabatic temperature change T_1 (Eq.(5.22)). So, the critical temperature gradient at that position $(\Delta T)_{crit} = T_1/x_1$ is large. If we replace u_1 by its expression

from Eq.(5.51), we get

$$x_1 = \frac{p_0}{\rho\omega a}\sin kx_s \quad (5.62)$$

Using Eq.(5.58) yields

$$x_1 = \frac{p_0}{\rho_m a^2}x_s \quad (5.63)$$

Substituting this result into Eq.(5.31)we obtain

$$(\Delta T)_{\text{crit}} = \gamma\frac{p_1 T_1}{p_0 x_s} = (\gamma - 1)\frac{T_1}{x_s} \quad (5.64)$$

where Eqs.(5.39) and (5.24) have been used. In the refrigerator (heat pump), $(\Delta T)_{crit}$ is the maximum temperature gradient that can be developed over the stack, which means that close to a pressure antinodes we can expect the largest temperature difference over the stack larger, so the maximum temperature difference that can be reached is smaller. Changes become smaller whereas displacements become larger, so the maximum temperature difference that can be reached is smaller.

V.IV.II. HEAT FLOW

Eq.(5.36) shows that the heat flow is proportional to the product p_1u_1, and so vanishes if the stack is placed at either a pressure node or a velocity node of the standing acoustic wave. The maximum value of $p_1u_1$is at $x = \lambda/8 = L/2$. The factor $(\Gamma - 1)$ appears also in the expression of heat flow. This factor is negative for refrigerators, and its effect can be derived from the discussion in preceding subsection. The lateral section of gas effective for the process $\Pi\delta_k$, can be maximized by using more plates, optimally spaced, in the stack so that the total perimeter Π is as large as possible while maintaining a stack spacing greater than about $2\delta_k$.

V.IV.III. ACOUSTIC POWER

In the absence of viscosity, the expression for the power needed to pump heat, Eq.(5.40), is similar to that of heat flow, the only difference is the presence of the work parameter $(\gamma - 1)$. Since each parcel along the plate absorbs net work, the total work done on the gas is proportional to the plate length L_s.

V.IV.IV. VISCOSITY

The discussion above concerns and in viscid gas. When viscosity is taken into account, the resulting expressions are much more complicated. These expressions will be presented in the following chapter.The viscous penetration depth is nearly as large as the thermal penetration depth, so most of the gas in the stack experiences significant viscous shear. However, the definition of the critical temperature gradient (Eq.(5.32)) will be kept throughout this thesis. In fact, with viscosity present, there is a lower critical temperature gradient below which the engine pumps heat and a higher critical gradient above which the engine is a prime mover. Between these two limiting gradients the engine is in a useless state, using work to pump heat from hot to cold.

V.IV.V. PERFORMANCE

At this stage, an estimation of the theoretical performance of the thermoacoustic devices, using an inviscid working gas, can be calculated from the expression of COP(η) derived in previous section in combination with the heat and work equations the COP is given by

$$COP = \frac{\dot{Q}}{\dot{W}} \tag{5.65}$$

Making use of Eqs.(5.32), (5.36), (5.38) and $\Delta T_m = \nabla T_m L_s$ yield

$$COP = \Gamma \frac{T_m}{\Delta T_m} = \Gamma\, COP_c \tag{5.66}$$

Here COP_C is Carnots coefficient of performance (Eq.(5.11)), the maximum possible performance of a refrigerator at T_m spanning the temperature difference ΔT_m. We see that COP_C is approached as $\Gamma \rightarrow 1$, in which case heat and work are zero.

We note that standing-wave thermoacoustic devices are intrinsically irreversible. The irreversible heat transfer δQ across the temperature difference δT, steps 2 and 4 in Fig.(5.3), is essential to the operation of these devices. They do rely on the imperfect thermal contact across the thermal penetration depth δk, which provides the necessary phasing between displacement and thermal oscillations. This is the reason why the performance of standing wave thermoacoustic devices falls below Carnot performance. The performance will be degraded furthermore if viscous, thermal conduction and other losses in the different parts of the device will be considered. To date, the best performance reached with such devices is about 20 % of Carnot.

VI. THEORY OF THERMOACOUSTICS

Although thermoacoustic phenomena are experimentally observed for over two centuries, it is only during the seventies that the general linear thermoacoustic theory has been developed by Rott and coworkers. The theory was first developed for heat generated oscillations (prime mover), but it is also applicable to thermoacoustic refrigerators and heat pumps. In this chapter the Rott's theory of thermoacoustics will be presented.

VI.I. GENERAL THERMOACOUSTIC THEORY

The thermoacoustic theory as known today is first developed by Rott and reviewed later by Swift. Starting with the linearization of the Navier-Stokes, continuity, and energy equations, we will proceed to develop the thermoacoustic equations avoiding much of the detail which has been provided elsewhere. For extended and detailed derivation of the different expressions, reference will be made to more specialized papers. The thermoacoustic equations are three fold: the first equation consists of Rott's wave equation, which is the wave equation for the pressure in the presence of a temperature gradient along the stack; the energy equation, which describes the energy flow in thermoacoustic systems; and the third equation that is an expression for the acoustic power absorbed (refrigerator) or produced (prime mover) in the stack. We will follow the notation used by Swift .The geometry used to derive and discuss the thermoacoustic equations is illustrated in Fig.(6.1). We consider a parallel-plate stack placed in a gas-filled resonator. The plates have a thickness 2l and gas spacing $2y_0$. The x axis is along the direction of acoustic vibration and the y axis perpendicular to the planes of the parallel plates,with $y = 0$ in the center of the gas-layer and $y = y_0$ at the gas-solid boundary. An y_0 axis is considered for the plates, with $y_0 = 0$ in the center of the plate and $y_0 = l$ at the boundary. So there are two opposite coordinate systems as indicated in Fig.(6.1).

Before beginning with writing the general equations of fluid mechanics, we will first summarize the assumptions which are used in deriving the general equations of thermoacoustics:

- The theory is linear, second-order effects other than energy transport, such as acoustic streaming and turbulence are neglected.
- The plates are stationary and rigid.
- The temperature spanned along the stack is much smaller than the absolute temperature.
- The temperature dependence of viscosity is neglected, which can be important at large temperature gradients.
- Oscillating variables have harmonic time dependence at a single angular frequency ω.

We note that sound results from a time-varying perturbation of dynamic and thermodynamic variables that describe the medium. a one-dimensional acoustic wave with an angular frequency ω exists, and the acoustic pressure is constant over the cross-sectional area of the stack, so that p = p(x).

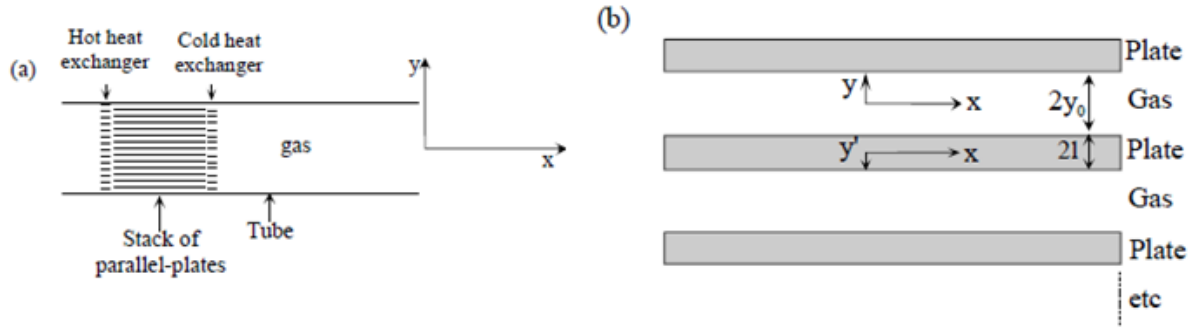

Figure 6.1: Geometry used for the derivation of thermoacoustic expressions. (a) Overall view, and (b) expanded view of the stack section. Each plate has thickness el, and each gas layer has thickness 2y

In thermoacoustics, a first order in the perturbations is considered for variables, and a second order in the perturbations for the energies. The fundamental physics concerned with thermoacoustics is described by Navier-Stokes continuity and energy equations

$$\rho\left[\frac{\partial v}{\partial t} + (v.\nabla)v\right] = -\nabla p + \mu\nabla^2 v + \left(\varepsilon + \frac{\mu}{3}\right)\nabla(\nabla.v) \quad (6.1)$$

$$\frac{\partial p}{\partial t} + \nabla.(\rho v) = 0 \quad (6.2)$$

$$\frac{\partial}{\partial t}\left(\frac{1}{2}\rho v^2 + \rho\varepsilon\right) = -\nabla.\left[\rho v\left(\frac{1}{2}v^2 + h\right) - k\nabla T - V.\Sigma\right] \quad (6.3)$$

where ρ is density, v is velocity, p is pressure, μ and ξ are dynamic (shear) and second(bulk) viscosity, respectively; K is the gas thermal conductivity, v^2 and h are internal energy and enthalpy per unit mass, respectively, and Σ is the viscous stress tensor with components

$$\Sigma_{ij} = \mu\left(\frac{\partial v_i}{\partial x_j} + \frac{\partial v_j}{\partial x_i} - \frac{2}{3}\delta_{ij}\frac{\partial v_k}{\partial x_k}\right) + \xi\delta_{ij}\frac{\partial v_k}{\partial x_k} \quad (6.4)$$

The temperature in the plates is given by the conduction equation

$$\frac{\partial T_s}{\partial t} = \frac{K_s}{\rho_s c_s}\nabla^2 T_s \quad (6.5)$$

where K_s, ρ_s and c_s are the thermal conductivity, the density and specific heat per unit mass of the stacks material, respectively. The temperature in the fluid is given can be derived from Eq.(6.3)

$$\rho T\left(\frac{\partial s}{\partial t} + v.\nabla_s\right) = K\nabla.(\nabla T) + \sigma'_{ik}\frac{\partial v_i}{\partial x_k} \quad (6.6)$$

The temperatures in the plates and in the gas are coupled at the solid-gas interface where continuity of temperature and heat fluxes is imposed. These conditions are respectively expressed as

$$T_1(y_0) = T_{01}(l) = T_b \quad (6.7)$$

$$K\,K\left(\frac{\partial T_1}{\partial y}\right)_{y0} = -K_0\left(\frac{\partial T_{01}}{\partial_{y'}}\right)_1$$

where subscript 1 indicates a first-order in the perturbation. The complex notation is used for time-oscillatory variables: pressure p, temperature T, velocity components (u, v,w), density ρ, and entropy per unit mass s

$$p = p_m + R_e[p_1(x)e^{jwt}] \quad (6.8)$$

$$u = R_e[u_1(x,y,z)e^{jwt}] \quad (6.9)$$

$$v, w = similar\ to\ u \quad (6.10)$$

$$T = T_m(x) + R_e[T_1(x,y,z)e^{jwt}] \quad (6.11)$$

$$\rho, s, T_0 = similar\ to\ T \quad (6.12)$$

In the acoustic approximation, the variables are harmonic and they have a $e^{j\omega t}$ time dependence, where ω = 2πf, and f is the oscillation frequency. The mean values of the different variables are given by the subscript m and are real. The first-order terms in the expansion which are complex are indicated by a subscript 1. We assume that this lowest order in the acoustic amplitude suffices for all

variables. Since δ_v, and λ are the characteristic lengths in x, y directions, respectively, and $\delta_v << \lambda$. This means that through this section we will always neglect $\partial/\partial x$ compared to $\partial/\partial y$. To first order, the x-component of the momentum equation can be written in the form

$$j\omega\rho_m u_1 = -\frac{d_{p1}}{d_x} + \frac{\partial^2 u_1}{\partial_{y^2}} + \left(\xi + \frac{\mu}{3}\right)\frac{\partial}{\partial_x}(\nabla . v_1) \quad (6.13)$$

where u_1 is the x component of v_1. Thus Eq.(6.13) reduces to

$$j\omega\rho_m u_1 = -\frac{d_{p1}}{d_x} + \mu\frac{\partial^2 u_1}{\partial_{y^2}} \quad (6.14)$$

With the boundary condition $u_1(y_0) = 0$, the solution u_1 of this equation can be written as the sum of the solution of the homogenous equation and a particular solution. The solution is

$$u_1(x,y) = \frac{j}{\rho_m\omega}\left(\frac{d_{p1}}{d_x}\right)\left[1 - \frac{\cosh\left[\frac{(1+j)}{\delta_v}y\right]}{\cosh\left[\frac{(1+j)}{\delta_v}y_0\right]}\right] \quad (6.15)$$

Where

$$\delta_v = \sqrt{\frac{2\mu}{\rho_m\omega}} \quad (6.16)$$

The parameter δv is the viscous penetration depth of the gas as defined in chapter 2.To first order, Eq.(6.5) becomes

$$j\omega T_{01} = \frac{K_0\partial^2 T_{01}}{\rho_0 c_0 \partial_{y'^2}} \quad (6.17)$$

Using the first boundary condition from expression (6.7), Eq.(6.17) has the solution

$$T_{01}(x,y') = \frac{\varepsilon_0}{(1+\varepsilon_0)}\left[\frac{\beta T_m}{\rho_m c_p}p_1 + \frac{dT_m}{\rho_{m\omega^2 d_x}}\left(\frac{d_{p1}}{d_x}\right)\left(\frac{1}{\sigma-1}\right)\left(1 - \frac{f_v}{\sigma f_k}\right)\right]\frac{\cosh(a_0 y')}{\cosh(a_0 l)} \quad (6.18)$$

Where

$$f_v = \frac{\tanh(a_v y_o)}{a_v y_0},\ a_v = \frac{(1+j)}{\delta_v} \quad (6.19)$$

$$f_k = \frac{\tanh(a_k y_o)}{a_k y_0},\ a_k = \frac{(1+j)}{\delta_k}$$

$$\varepsilon_0 = \frac{\sqrt{K\rho_m c_p}}{\sqrt{K_0\rho_0 c_0}}\frac{\tanh(a_k y_0)}{\tanh(a_0 l)},\ a_0 = \frac{(1+j)}{\delta_0}$$

And

$$\delta_k = \sqrt{\frac{2K}{\rho_m c_p \omega}} \quad (6.20)$$

$$\delta_0 = \sqrt{\frac{2K}{\rho_0 c_0 \omega}} \quad (6.21)$$

$$\sigma = \left(\frac{\delta_v}{\delta_k}\right)^2 \quad (6.22)$$

where δk is the thermal penetration depth of the gas, δs is the solids thermal penetration depth, and σ is the Prandtl number. The function f is the so called Rotts function and it is geometry dependent. Using the thermodynamic expression

$$d_s = \left(\frac{c_p}{T}\right)dT - \left(\frac{\beta}{\rho}\right)d_p \quad (6.23)$$

where c_p and β are the specific heat per unit mass and the isobaric thermal expansion coefficient of the gas, respectively. To first order, Eq.(6.6) becomes

$$\rho_m c_p\left(j\omega T_1 + u_1\frac{dT_m}{d_x}\right) - j\omega\beta T_m p_1 = K\frac{\partial^2 T_1}{\partial_{y^2}} \quad (6.24)$$

Substituting Eq.(6.15) for u_1, and solving Eq.(6.24) for T_1, with the boundary condition of Eq.(6.7). The solution is

$$T_1(x,y) = \frac{\beta T_m}{\rho_m c_p}p_1 - \frac{dT_m d_{p1}}{\rho_m\omega^2 d_x d_x}\left(1 - \left[\left(\frac{\sigma}{\sigma-1}\right)\frac{\cosh(a_v y)}{\cosh(a_v y_0)}\right]\right)$$
$$-\left(\frac{\beta T_m}{\rho_m c_p}p_1 + \frac{\left(1 + \frac{c_0 f_v}{f_k}\right)dT_m d_{p1}}{\rho_m\omega^2(\sigma-1)d_x d_x}\right)\frac{\cosh(a_k y)}{(1+\varepsilon_0)\cosh(a_v y_0)} \quad (6.25)$$

For the derivation of Rott's wave equation, we begin with the continuity equation, Eq.(6.2), which to first order becomes

$$j\omega\rho_1 + \frac{\partial}{\partial_x}(\rho_m u_1) + \rho_m\frac{\partial_{v1}}{\partial_y} = 0 \quad (6.25)$$

By combining this equation with the x derivative of Eq.(6.14), one obtains

$$-\omega^2\rho_1 - \frac{d^2 p1}{d_{x^2}} + \frac{\partial}{\partial_x}\left(\mu\frac{\partial^2 u1}{\partial_{y^2}}\right) + j\omega\rho_m\frac{\partial_{v1}}{\partial_y} = 0 \quad (6.26)$$

The density ρ_1 is related to T_1 and p_1 by the thermodynamic expression

$$\rho_1 = \rho_m \beta T_1 + \left(\frac{\gamma}{a^2}\right) p_1 \tag{6.28}$$

where γ is the ratio of isobaric to isochoric specific heats and a is the adiabatic sound speed. Substituting Eq.(6.28) into Eq.(6.27), yields

$$\rho_m \beta \omega^2 T_1 - \frac{\omega^2}{a^2}\gamma p_1 - \frac{d^2 p1}{d_{x^2}} + \frac{\partial}{\partial x}\left(\mu \frac{\partial^2 u1}{\partial y^2}\right) + j\omega\rho_m \frac{\partial v1}{\partial y} = 0 \tag{6.29}$$

By incorporating Eqs.(6.25) and (6.15) into Eq.(6.29), and integrating with respect to y from 0 to y_0, we obtain the wave equation of Rott

$$\left[1 + \frac{(\gamma-1)}{(1+\varepsilon_0)} f_k\right] p_1 + \frac{a^2}{\omega^2}\rho_m \frac{d}{dx}\left[\frac{(1-fv)dp1}{\rho_m dx}\right] + \frac{a^2}{\omega^2}\frac{(fk-fv)}{(\sigma-1)(1+\varepsilon_0)}\beta \frac{dT_m dp1}{dx\, dx} = 0 \tag{6.30}$$

This is the wave equation for p_1 in the presence of a mean temperature gradient dT_m/dx in the stack. For an ideal gas and ideal stack with $\varepsilon_s = 0$, this result was first obtained by Rott. Now, we will proceed to develop an expression for the time-averaged acoustic power dW used (or produced in the case of a prime mover) in a segment of length *dx* in the stack. This power is the difference between the average acoustic power at *x+dx* and x, thus

$$d\dot{W} = A_g\left[\overline{(p_1 u_1)}_{x+dx} - \overline{(p_1 u_1)}_x\right] \tag{6.31}$$

where over bar indicates time average, brackets indicate averaging in the y direction, and A_g is the cross-sectional area of the gas within the stack. Expanding $\overline{(p_1 u_1)}_{x+dx}$ in a Taylor series, and p being independent of y, Eq.(6.31) can be written as

$$dW = A_g\left[\frac{\overline{dp1(u1)}}{dx} dx\right] \tag{6.32}$$

The time average of the product of two complex quantities such as p_1 and u_1 is given by

$$\overline{p_1(u_1)} = \frac{1}{2} R_e[p_1(u_1)] \tag{6.33}$$

where the star denotes complex conjugation and signifies the real part. Using Eq.(6.33) and expanding the derivatives in Eq.(6.32) gives

$$d\dot{W} = \frac{1}{2} A_g R_e\left[p_1 \frac{d(u_1)}{dx} + (u_1)\frac{dp_1}{dx}\right] dx \tag{6.34}$$

To evaluate this expression, the derivatives dp_1/dx and $\frac{d(u_1)}{dx}$ are needed. The expression for dp_1/dx is obtained from Eq.(6.15), as follows

$$(u_1) = \frac{j}{\rho_m \omega}\frac{d_{p1}}{dx}(1 - fv) \tag{6.35}$$

so that

$$\frac{d_{p1}}{dx} = \frac{-j\rho_m \omega(u1)}{(1-f_v)} \tag{6.36}$$

The derivative dp_1/dx can be obtained from the second term in Rott's wave equation and Eq.(6.35), as follows

$$\frac{a^2}{\omega^2}\rho_m \frac{d}{dx}\left[\frac{(1-fv)}{\rho_m}\frac{d_{p1}}{dx}\right] = \frac{a^2}{\omega^2}\rho_m \frac{d}{dx}\left(-j\omega(u_1)\right) \tag{6.37}$$

Substituting this into Eq.(6.30) produces

$$\frac{d(u_1)}{dx} = \frac{-jw}{\rho_m a^2}\left[1 + \frac{(\gamma-1)}{(1+\varepsilon_0)} f_k\right] p_1 + \frac{(f_k - f_v)}{(1-\sigma)(1+\varepsilon_0)(1-f_v)}\beta \frac{dT_m}{dx}(u_1) \tag{6.38}$$

Substituting Eqs.(6.36) and (6.38) into Eq.(6.34) yields

$$\frac{dW_2}{dx} = -\frac{1}{2} A_g \omega\left(\frac{\rho_m Im(-f_v)}{|1-f_v|^2}|(u_1)|^2 + \frac{(\gamma-1)Im(-f_k)}{\rho_m a^2(1+\varepsilon_0)}|p_1|^2\right) + \frac{1}{2} A_g \omega\left(\frac{\beta}{\omega(1-\sigma)(1+\varepsilon_0)}\frac{dT_m}{dx} R_e\left(\frac{(f_k - f_v)}{(1-f_v)} p_1(u_1)\right)\right) \tag{6.39}$$

This is the acoustic power absorbed (or produced) in the stack per unit length. The subscript 2 is used to indicate that the acoustic power is a second-order quantity; the product of two first-order quantities, p_1 and u_1.

The first two terms in Eq.(6.39), are the viscous and thermal relaxation dissipation terms, respectively. These two terms are always present whenever a wave interacts with a solid surface, and have a dissipative effect in thermoacoustics. The third term in Eq.(6.39) contains the temperature gradient dT_m/dx. This term can either absorb (refrigerator) or produce acoustic power (prime mover) depending on the magnitude of the temperature gradient along the stack. This term is the unique contribution to themoacoustics.

Finally, we will now proceed to develop an expression for the time-averaged energy Flux E_2 in the stack, correct to second-order in the acoustic variables. We consider the thermoacoustic refrigerator shown in Fig(6.1a), driven by a loudspeaker. We suppose that the refrigerator is thermally insulated from the surroundings except at the two heat exchangers, so that heat can be exchanged with the outside world only via the two heat exchangers. Work can be exchanged only at the loudspeaker piston. The general law of conservation of energy for a fluid, where there is viscosity and thermal conduction is given by Eq.(6.3), is expressed by Eq.(6.40) below

$$\frac{\partial}{\partial t}\left(\frac{1}{2}\rho v^2 + \rho\epsilon\right) = -\nabla.\left[v.\left(\frac{1}{2}\rho v^2 + \rho h\right) - \mathrm{k}\nabla\mathrm{T} - \mathrm{v}.\Sigma\right] \tag{6.40}$$

where ε and h are the internal energy and enthalpy per unit mass, respectively, and Σ is the viscous stress tensor, with components given by Eq.(6.4). The expression on the left is the rate-of-change of the energy in unit volume of the fluid, while that on the right is

the divergence of the energy flux density which consists of three terms: transfer of mass by the motion of the fluid, transfer of heat and energy flux due to internal friction, respectively.

In steady state, for a cyclic refrigerator (prime mover) without heat flows to the surroundings, the time averaged energy flux E_2 along x must be independent of x. Terms of third order in v are neglected. Taking the x component of Eq.(6.40), integrating the remaining terms with respect to y from y = 0 to y = y_0, and time averaging yields

$$\frac{d\left[\int_0^{y_0}\overline{\rho uh}dy-\int_0^{y_0}k\overline{\frac{\partial T}{\partial x}}dy-\int_0^{l}K_s\overline{\frac{\partial T_s}{\partial x}}dy'-\int_0^{y_0}\overline{v.\Sigma}\ dy\right]}{dx}=0 \tag{6.41}$$

The quantity within the square brackets is the time-averaged energy flux per unit
Perimeter E_2/Π along x

$$\frac{\dot{E_2}}{\Pi}=\int_0^{y_0}\overline{\rho uh}\,dy-\int_0^{y_0}\overline{k\frac{\partial T}{\partial x}}\,dy-\int_0^{l}\overline{K_s\frac{\partial T_s}{\partial x}}dy'-\int_0^{y_0}\overline{v.\Sigma}\ dy \tag{6.42}$$

Using the acoustic approximations Eqs.(6.8)-(6.12), keeping terms up to second order the first integral in Eq.(6.42) becomes

$$\overline{\rho uh}\ \simeq\ \rho_m h_m\overline{u_1}+\rho_m h_m\overline{u_2}+\rho_m\overline{h_1u_1}+h_m\overline{\rho_1u_1} \tag{6.43}$$

The first term on the right in Eq.(6.43) is zero because $u_1 = 0$. The integrals of the second and third terms in Eq.(6.43) sum to zero because the second-order time- averaged mass flux is zero

$$\overline{p_1u_1}+\rho_m\overline{u_1}=0 \tag{6.44}$$

Hence, if we use the thermodynamic expression

$$dh=Tds+\frac{dp}{\rho}=c_p dT+\left(\frac{1}{\rho}\right)(1-\beta T)dp \tag{6.45}$$

we obtain

$$\overline{\rho uh}\ \simeq\ \rho_m\overline{h_1u_1}=\ c_p\rho_m\overline{T_1u_1}+(1-\beta T_m)\overline{p_1u_1} \tag{6.46}$$

The largest term in the last integral in Eq.(6.42) is of order $y_0\mu u_1/\lambda$; but the term ρuh, in the first integral, is of order $p_1u_1 \sim \rho_m a u_1^2$, so that the last integral can be neglected. Only the zero-order terms are significant in the second and third integrals in Eq.(6.42). Hence Eq.(6.42) becomes

$$\frac{\dot{E_2}}{\Pi}=\int_0^{y_0}\rho_m\overline{h_1u_1}\,dy-(y_0K+lK_s)\frac{dT_m}{dx} \tag{6.47}$$

$$=\int_0^{y_0}\overline{p_1u_1}\,dy+\int_0^{y_0}T_m\rho_m\overline{s_1u_1}\,dy-(y_0K+lK_s)\frac{dT_m}{dx} \tag{6.48}$$

so that

$$\frac{\dot{E_2}}{\Pi}=\int_0^{y_0}\left[c_p\rho_m\overline{T_1u_1}+(1-\beta T_m)\overline{p_1u_1}\right]dy-(y_0K+lK_s)\frac{dT_m}{dx} \tag{6.49}$$

The subscript 2 is again used to indicate that the energy flux is second order in the acoustic quantities. Substituting Eq.(6.15) for u_1 and Eq.(6.25) for T_1 and performing the integration yields finally

$$E_2=\frac{A_g}{2}R_e\left[p_1\langle u_1^*\rangle\left(1-\frac{\beta T_m(f_k^*-f_v^*)}{(1+\sigma)(1+\varepsilon_s)(1-f_v^*)}\right)\right]+\frac{A_g\rho_m c_p|\langle u_1\rangle|^2}{2\omega(1-\sigma)(1+\varepsilon_s)|1-f_v|^2}\frac{dT_m}{dx}Im\left[f_v^*+\frac{(f_k^*-f_v^*)(1+\frac{e_0f_v}{f_k})}{(1+\varepsilon_s)(1+\sigma)}\right]-\left[A_gK+A_sK_s\right]\frac{dT_m}{dx} \tag{6.50}$$

where A_s is the cross-sectional area of the stack material. This important result represents the energy flux along x direction (wave direction) in terms of $T_m(x)$, $p_1(x)$, material properties and geometry. For an ideal gas and ideal stack $\varepsilon_s = 0$, this result was first obtained by Rott . As can be seen from Eq.(6.47), the energy flux consists of three terms: the first term in p_1u_1 is the acoustic power, the second term in s_1u_1 is the hydrodynamic entropy flow, and the final term is simply the conduction of heat through gas and stack material in the stack region. As discussed before, the time-averaged energy flux $\dot{E}_2$ along the stack must be independent of x. With $\dot{E}_2$ constant, we solve Eq.(6.50) for dT_m/dx, so that T_m can be evaluated

$$\frac{dT_m}{dx}=\frac{\left\{\frac{\dot{E_2}}{A_g}-\frac{1}{2}R_e\left[p_1\langle u_1^*\rangle\left(1-\frac{(f_k^*-f_v^*)}{(1+\sigma)(1+\varepsilon_s)(1-f_v^*)}\right)\right]\right\}}{\left\{\frac{\rho_m c_p|\langle u_1\rangle|^2}{2\omega(1-\sigma)(1+\varepsilon_s)|1-f_v|^2}Im\left[f_v^*+\frac{(f_k^*-f_v^*)(1+\frac{e_0f_v}{f_k})}{(1+\varepsilon_s)(1+\sigma)}\right]-K-\frac{A_0}{A_g}K_0\right\}} \tag{6.51}$$

As can be seen from Eqs.(6.39) and (6.50), the expressions for the acoustic energy flows are complicated and difficult to interpret. But they are useful for numerical calculation.

In summary Eqs.(6.36), (6.38), and (6.51) form a system of have coupled equations because the two first equations are complex. These equations which represent the have real variables: $R_e(p_1)$, $I_m(p_1)$, Re ($<u_1>$), $I_m(<u_1>)$, and T_m, incorporate the physics of the thermoacoustic effect; and can be used for analysis and design of thermoacoustic systems.

VI.II. BOUNDARY LAYER AND SHORT-STACK APPROXIMATIONS

The thermoacoustic expressions derived in the previous section are complicated to interpret. In this section we will use two assumptions, to simplify these expressions. First, we make use of the .boundary-layer. Approximation: $y_0 >> \delta K$, $l >> \delta s$, so that the hyperbolic tangents in Eq.(6.19)can be set equal to unity. Second, we make the short-stack. Approximation, $L_s << \lambda$; where the stack is considered to be short enough that the pressure and velocity in the stack does not vary appreciably. Finally, we will consider standing-wave systems, which are more related to the experimental work in this study.

The standing wave acoustic pressure in the stack p_1^s, can be taken as real and is given by

$$p_1 = p_1^s = p_0 \cos(kx) \tag{6.52}$$

and the mean gas velocity in x direction is

$$\langle u_1 \rangle = j\left(1 + \frac{l}{y_0}\right)\frac{p_0}{\rho_m a}\sin(kx) = j\langle u_1^s \rangle \tag{6.53}$$

The superscript s refers to standing waves, p_0 is the pressure amplitude at the pressure antinodes of the standing wave and k is the wave number. The factor $(1+l/y_0)$ is used because of the continuity of the gas volumetric velocity at the boundary of the stack which requires that the velocity inside the stack must be higher than that outside by the cross-sectional area ratio $(1 + l/y_0)$. The Rott's function *f* in the boundary layer-approximation is given by

$$f = \frac{(1-j)\delta}{y_0} \tag{6.54}$$

Using these assumptions and $A_g = \Pi_{y0}$, $A_s = \Pi l$; the approximate expressions for $\dot{W}_2$ and $\dot{E}_2$ are obtained, respectively.

$$\dot{W}_2 = \frac{1}{4}\Pi\delta_k L_s \frac{(\gamma-1)\omega(p_1^s)^2}{\rho_m a^2(1+\varepsilon_s)}\left(\frac{\Gamma}{(1+\sqrt{\sigma})\Lambda} - 1\right) - \frac{1}{4}\Pi\delta_v L_s \frac{\omega\rho_{m\langle u_1^s\rangle^2}}{\Lambda} \tag{6.55}$$

And

$$\dot{E}_2 = -\frac{1}{4}\Pi\delta_k \frac{\beta T_m p_1^s \langle u_1^s \rangle}{(1+\gamma)(1+\varepsilon_s)\Lambda}\left[\left[\Gamma\frac{1+\sqrt{\sigma}+\sigma+\sigma\varepsilon_s}{1+\sqrt{\sigma}} - \left(1+\sqrt{\sigma}-\frac{\delta_v}{y_0}\right)\right] - \Pi[y_0 K + lK_s]\frac{dT_m}{dx}\right. \tag{6.56}$$

Where

$$\Lambda = 1 - \frac{\delta_v}{y_0} + \frac{\delta_v^2}{2y_0^2} \tag{6.57}$$

In Eq.(6.55), L_S is the stack length, Π is the total perimeter of the stack plates in the direction normal to the x axis, and $\Pi\delta k L_S$ is the volume of gas within about a thermal penetration depth from the plates. $\Gamma = \nabla T_m/\nabla T_{crit}$, and ∇T_{crit} is given by Eq.(2.32)

$$\nabla T_{crit} = \frac{\beta T_m \omega p_1^s}{\rho_m c_p \langle u_1^s \rangle} \tag{6.58}$$

The second term on the right hand side of Eq.(6.55) and the second term between brackets (−1) are negative and are the viscous and thermal relaxation dissipation terms, respectively. These two terms have a dissipative effect on the performance of thermoacoustic devices. The first term between brackets on the right hand side of Eq.(6.55), proportional to Γ, is the acoustic power absorbed to transfer heat ($\Gamma < 1$)or produced in the case of a prime mover ($\Gamma > 1$). We note again that the acoustic power W_2 and energy E_2 are quadratic in the acoustic amplitude. Furthermore, W_2 is proportional to the volume $\Pi\delta_k L_S$ of gas that is located within δk from the stack surface.

As will be shown in the next section, the E_2 is the heat removed from the cold heat exchanger in our refrigerator. The first term on the right hand side of Eq.(6.56) is the thermoacoustic heat flow. The second term on the right hand side of Eq.(6.56) is simply the conduction of heat through gas and stack material in the stack region. So that the heat conduction has also have a negative effect on the performance of thermoacoustic refrigerators. The energy flow E_2 is proportional to the area $\Pi\delta_k$, which is the cross- sectional area of gas that is at δk from the stack surface. If $\delta k \sim y_0$, essentially the entire cross-sectional area of gas in the stack participates in the thermoacoustic heat transport. The energy flow is also proportional to the product $p_i\langle u_i \rangle$. Equations (6.55) and (6.56) contain the important parameter Γ which determines the sign of this expressions and hence the mode of operation of the apparatus, as discussed previously. Substituting Eqs.(6.52) and (6.53) into Eq.(6.58), we obtain

$$\nabla T_{crit} = \frac{(\gamma-1)}{\left(1+\frac{l}{y_0}\right)} kT_m \cot(kx) \tag{6.59}$$

Eq.(6.59), shows that the critical temperature gradient is independent of the acoustic amplitude for a given location of the stack center within the standing wave. We see from Eq.(6.55) and Eq.(6.56), that the energy flow and acoustic power depend on of the Prandtl number σ (viscosity), in a complicated way. The influence of the Prandtl number on $\dot{W}_2$ and $\dot{E}_2$ and hence on the performance of the refrigerator will be discussed in the next section.

VI.III. ENERGY FLUXES IN THERMOACOUSTIC REFRIGERATOR

In the preceding sections, expressions for the acoustic power W2 absorbed in a thermoacoustic refrigerator or produced in a prime mover and the total energy flow E_2 in the system have been presented. As can be seen from Eq.(6.47), the total energy is the

sum of the acoustic power (first term), the hydrodynamic heat flux (second term) and the conduction heat flux. An idealized illustration of the different flows and their interplay in a thermoacoustic refrigerator will be given in this section.

Fig.(6.2a) shows a standing wave refrigerator thermally insulated from the surroundings except at the heat exchangers where heat can be exchanged with the surroundings. The arrows show the different energy flows into or out of the system except the conductive heat flow which is neglected for ease of discussion. A loudspeaker (driver) sustains a standing acoustic wave in the resonator by supplying acoustic power W_2 in the form of a travelling acoustic wave. A part of this power will be used to sustain the standing wave against the thermal and viscous dissipations, and the rest of power will be used by the thermoacoustic effect to transport heat from the cold heat exchanger to the hot heat exchanger, as discussed previously using Eq.(6.55).

In Fig.(6.2b), An idealized energy diagram, illustrating the behavior of the different energy flows as function of the position, is given. A part of the acoustic power delivered by the loudspeaker is dissipated at the resonator wall (first and second term in Eq.(6.39)), to the left and right of the stack. The dissipated part to the right of the cold heat exchange shows up as heat at the cold heat exchanger. This will decrease the effective cooling power of the refrigerator. The acoustic power in the stack and heat exchangers decreases monotonously, as it is used to transport heat from the cold heat exchanger to the hot heat exchanger, and to overcome the viscous forces in the stack.

This used power shows up as heat at the hot heat exchanger. The power dissipated at the tube wall to the left of the stack will also show up at the hot heat exchanger .Within the stack, the heat flux grows from $\dot{Q}_H$ at the left end of the stack to $\dot{Q}_H$ at the right end. The two discontinuities in the heat flux are at the two heat exchangers at T_C and T_H, supplying heat $\dot{Q}_C$ and removing heat $\dot{Q}_H$. The total energy flow is everywhere the sum of acoustic work and heat fluxes. Within the stack the total energy is constant. The heat flux rises while acoustic power decreases, so that conservation of energy holds.

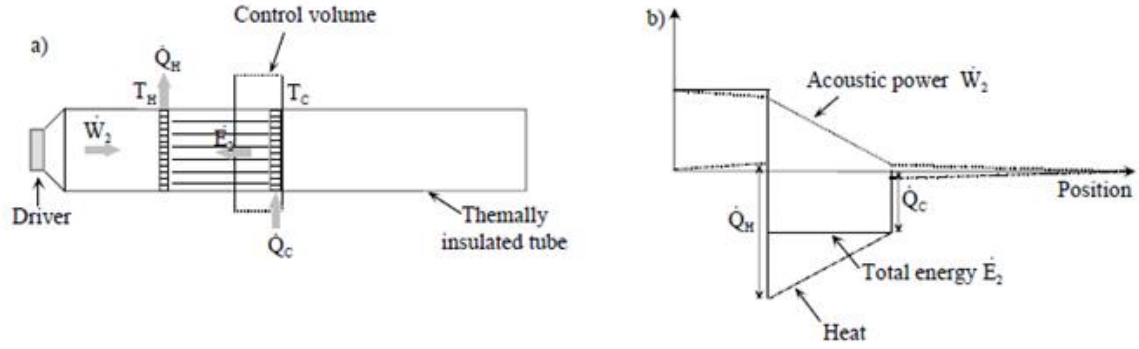

Figure 6.2: a) A standing wave refrigerator, insulated everywhere wxept at the heat exchangers. B) Illustration of W_2,Q_2 and E_2 in the refrigerator. The discontinuities in E_2 are due to heat transfer at the heat exchangers.

If we apply the principle of energy conservation to the control volume shown by the dotted line in Fig.(6.2a), in steady state over a cycle, the energy inside the control volume cannot change, so that the rate at which energy flows out is $\dot{E}_2$ and the rate at which energy flows in is $\dot{Q}_C$, we conclude that $\dot{Q}_C$ is equal to $\dot{E}_2$.

VI.IV. NON-LINEAR EFFECTS

The thermoacoustic theory developed so far is based on the acoustic approximation. Hence only small amplitudes were supposed. Actually, thermoacoustic devices developed for practical use will always operate at high amplitude. Hence, one may expect that non-linear effects will be present in such systems. This section is intended to give a short survey of some non-linear effects. A detailed review of these effects can be found in the text of Swift . A short review of turbulence, and streaming will be given. Since these effects dissipate acoustic power, they have a negative effect on the performance of thermoacoustic devices.

VI.IV.I. TURBULENCE

From many experimental studies on the structure of turbulent oscillatory flows, it has unanimously been observed that transition to turbulence in the boundary layer took place at a Reynolds number (R^{δ_v}) based on Stokes boundary-layer thickness of about 500 to 550, independent of the particular flow geometry (pipe, channel, oscillating plate) . The Reynolds number is defined as

$$R^{\delta_v} = \frac{\langle u_1 \rangle \varepsilon_v \rho}{\mu} \qquad (6.60)$$

here u_1 is the average velocity given by Eq.(6.35).

The transition between laminar and turbulent regimes for an oscillating flow in atube of radius r, occurs roughly at

$$R_y \simeq 2000 \; for \; r < 2\delta_v$$

$$\frac{R_y}{\frac{r}{\delta_v}} \simeq 1000 \; for \; r > 2\delta_v \tag{6.61}$$

Where

$$R_y = \frac{u_1 D \rho}{\mu} \tag{6.62}$$

is the Reynolds number based on the diameter of the tube D, and the peak acoustic velocity u_1.

VI.IV.II. STREAMING

The word streaming refers to second-order steady flow, which is superimposed on the first-order acoustic oscillatory flow. Streaming is driven by first-order acoustic phenomena (c.f. Eq.(6.44)). The streaming has a negative effect on the performance of the thermoacoustic devices, because it generates a convective heat transport. In a refrigerator such convective heat adds an undesirable heat load on the cold heat exchanger. In an engine this effect wastefully removes heat from the hot heat exchanger without generating acoustic power. Many types of streaming exist depending on the driving cause: Gedeon streaming is a DC flow which may exists whenever a toroidal geometry is used. Rayleigh streaming occurs in tubes and is driven by the viscous and thermal boundary-layers phenomena at the side walls of the tube. A streaming is set upward near the walls of the tube and downwards in the central part of the tube (or vice versa). This streaming can be eliminated by using a tube with variable crossection. Toroidal streaming may also occur in the stack. Gravity driven convection is also another type of streaming which may be avoided by orienting the cold side of the system downward.

VI.IV.III. HARMONICS AND SHOCKS

Harmonics can be generated in thermoacoustic devices by non-linear phenomena, like the v.∇v term in the Navier-Stokes equation. In such case the fundamental mode, u_1, interacts with its derivative to generate higher modes. As will be shown in proceeding section, some resonator geometries can be used to avoid that the higher resonator modes which occur at frequencies that are an integer multiple of the fundamental mode frequency ω, so that the cascade excitation of the higher modes by non-linearities may be avoided. Shock waves can also occur at very high amplitudes as a consequence of interactions between the different modes. Harmonics and shock waves can be easily detected using an oscilloscope.

VII. DESIGN OF A THERMOACOUSTIC REFRIGERATOR

This section is concerned with the design, development and optimization of thermo acoustic refrigerators using readily available materials. The linear thermo acoustic theory presented in previous section will be used. Due to the large number of parameters, a choice of some parameters along with a group of dimensionless independent variables will be used. The optimization of the different parts of the refrigerator will be discussed, and likewise some criteria will be implemented to obtain an optimal system.

VII.I DESIGN STRATEGY

As discussed in the previous section, thermo acoustic refrigerators consist mainly of four parts: a driver, a stack, two heat exchangers, and a resonator (Fig. (3.3)). Our approach to the design and optimization of the refrigerator consists of the design and optimization of each part separately. In this section the optimization and design of the other modules will be considered.

We start by considering the design and optimization of the stack. As can be seen from Eq.(6.55) the driver has to provide acoustic power for driving the thermo acoustic heat transport process and for compensating for all viscous and thermal dissipation processes in the stack, heat exchangers, and at the resonator wall. The coefficient of performance of the stack, defined as the ratio of the heat pumped by the stack to the acoustic power used by the stack, is the maximum performance of the refrigerator. The exact expressions, Eqs.(6.39) and (6.50), of the acoustic power and cooling power in the stack are complicated, so one can try to use the expressions deduced from the short stack, and boundary-layer approximations, Eqs.(6.55) and (6.56). These expressions still look complicated.

They contain a large number of parameters of the working gas, material and geometrical parameters of the stack. It is difficult to deal in engineering with so many parameters. However, one can reduce the number of parameters by choosing a group of dimensionless independent variables. Olson and Swift wrote a paper about similitude and dimensionless parameters for thermo acoustic devices .Some dimensionless parameters can be deduced directly from Eqs.(6.55) and (6.56).Others can be defined from the boundary-layer and short-stack assumptions. The parameters, of importance in thermo acoustics, which are contained in Eqs.(6.55) and(6.56), are given in Tables (7.1) and (7.2).

Table 7.1: Operation and working gas parameters

Operation parameters	Working gas parameters
Operating frequency: f Average pressure: p_m Mean temperature: T_m	Dynamic viscosity: μ Thermal conductivity: K Sound velocity: a Ratio of isobaric to isochoric specific heats: γ

Table 7.2: Parameters of the stack

Material	Geometry
Thermal conductivity: K_s Density: ρ_s Specific heat: c_s	Length: L_s Stack center position: x_s Plate thickness: 2l Plate spacing: 2_{y0} Cross section: A

The goal of the proper design of the thermo acoustic refrigerator is to meet the requirements of a given cooling power Q_c and a given low temperature T_c or a given temperature difference ΔT over the stack. This requirement can be added to the operation parameters shown in Table 7.1.

As discussed earlier, the boundary layer and short stack approximations assume the following:

- The reduced acoustic wavelength is larger than the stack length: $\lambda/2\pi = 1/k >> Ls$, so that the pressure and velocity can be considered as constant over the stack and that the acoustic field is not significantly disturbed by the presence of the stack.
- The thermal and viscous penetration depths are smaller than the spacing in the stack: δ_k, $\delta_v << y_0$. This assumption leads to the simplification of the Rott.s functions, where the complex hyperbolic tangents can set equal to one (Eqs.(6.19)).
- The temperature difference is smaller than the average temperature: $\Delta T << T_m$, so that the thermo physical properties of the gas can be considered as constant within the stack

The length and position of the stack can be normalized by $\lambda/2\pi$. The thermal and viscous penetration depths can be normalized by y_0. The cold temperature or the temperature difference can be normalized by Tm. Since δ_k, and $\delta_v$are related by the Prandtl number σ, this will further simplify the number of parameters. Olsonand Swift proposed to normalize the acoustic power and the cooling power by the product of the mean pressure p_m, the sound velocity a, and the cross-sectional area of the stack A : $p_m aA$. The amplitude of the dynamic pressure can be normalized by the mean pressure. The ratio p_0/ p_m is called the drive ratio: D. In practice the stack material can be chosen so that ε_s and the thermal conductive term in Eqs.(6.55) and(6.56) can be neglected. In this case the parameters of the stack material don't have to be considered in the performance calculations. The porosity of the stack, sometimes called blockage ratio, defined as

$$B = \frac{y_0}{y_0 + l} \qquad (7.1)$$

is also used as a dimensionless parameter for the geometry of the stack. The resultant normalized parameters are given an extra index n and are shown in Tables (7.3)-(7.5). The number of parameters can once more be reduced, by making a choice of some operation parameters, and the working gas

Table 7.3: Normalized operation parameters

Operation parameters
Drive ratio: $D = p_1/p_m$
Normalized cooling power: $Q_{cn} = Q_c/p_m aA$
Normalized acoustic power: $W_n = W/p_m aA$
Normalized temperature difference: $\Delta T_{mn} = \Delta T_m/T_m$

Table 7.4: Normalized gas parameters

Gas parameters
Prandtl number: σ
Normalized thermal penetration depth: $\delta_{kn} = \delta_k/y_0$

Table 7.5: Normalized stack parameters

Stack geometry parameters
Normalized stack length: $L_{sn} = kL_s$
Normalized stack position: $x_n = k_x$
Blockage ratio or porocity: $B = \frac{y_0}{y_0 + l}$

VII.II. DESIGN CHOICES

For this investigation we choose to design a refrigerator for a temperature difference of $\Delta T_m = 75$ K and a cooling power of 4 watt. In the following, we will discuss the selection of some operation parameters, the gas, and stack material.

Average pressure:

Since the power density in a thermo acoustic device is proportional to the average pressure p_m it is favorable to choose p_m as large as possible. This is determined by the mechanical strength of the resonator. On the other hand, δ_k is inversely proportional to square root of p_m, so a high pressure results in a small δ_k and very small stack plate spacing. This makes the construction difficult. Taking into account these effects, we choose to use 1bar. To minimize the heat conduction from the hot side of the stack to the cold side, we used a thin-walled stack holder made of a Ertacetal material.

Frequency:

As the power density in the thermo acoustic devices is a linear function of the acoustic resonance frequency an obvious choice is thus a high resonance frequency. On the other hand δ_k is inversely proportional to the square root of the frequency (Eq.(5.46))which again implies a stack with very small plate spacing making a comprise between these two effects and the fact that the driver resonance has to be matched to the resonator resonance for high efficiency of the driver, we choose to use a frequency of 400 Hz.

Drive ratio:

The drive ratio,D , is defined as the acoustic pressure amplitude, P_1, divided by the mean pressure ,P_m . This ratio should be kept sufficiently low so as to avoid acoustic nonlinearities such as turbulence. Specifically, the dimensionless Mach number, *M*, should be smaller than about 0.1, and the Reynolds number, R_y, should be smaller than 500. The following definition of the Mach number:

$$M = \frac{D}{\gamma}$$

This formulation seems to be better suited for use with the dimensionless equations in designing the stack. Given, γ =1.43, the drive ratio must be less than 14.3% to ensure that and less than 10.0% to ensure that $R_y < 500$. Because the chosen mean pressure is 1 bar, the acoustic pressure amplitude must be less than 0.1 bar, a large number for a normal loud speaker, the intended driver. The actual drive ratio for a loud speaker is more likely to be on the order of a few percent. Therefore, to proceed with calculations it was assumed that $D = 0.01$ so that the actuator would not need to be driven excessively hard to achieve the calculated cooling power and efficiency.

Dynamic pressure:

The dynamic pressure p_0 is limited by two factors namely, the maximum force of the driver and non-linearities. The acoustic Mach number, defined as

$$M = \frac{p_0}{\rho_m a^2} \qquad (7.2)$$

has to be limited to M ~ 0.1 for gases by nonlinear effects . It was indicated in previous section that in order to avoid turbulence the acoustic Reynolds number $R_y^{\delta v}$,Eq.(6.60), should be smaller than 500. Since we intend to design a refrigerator with moderate cooling power we will use driving ratios D < 3 %, so that M < 0.1 and $R_y^{\delta v} < 500$.

Working gas:

We use atmospheric air as working gas. In this way the resonance frequency of 400 Hz is easily obtained without making the system too small. It is cheap in comparison with the other other gases. A high thermal conductivity is wise since δk is proportional to the square of the thermal conductivity coefficient K. The effect of using other gases will be discussed later in this Chapter.

Stack material:

The second term in Eq.(6.56) represents the heat conductivity through the stack material and gas in the stack region. This heat conduction has a negative effect on the performance of the refrigerator. The stack material must have a low thermal conductivity K_s and heat capacity c_s larger than the heat capacity of the working gas, in order that the temperature of the stack plates is steady. In this way the parameter can be neglected. The material Teflon is chosen, as it has a low heat conductivity (0.16 W/mK) and is produced in thicknesses of 10 μm-500 μ_m .

Stack geometry:

There is much geometry which the stack can have: Parallel plates, circular pores, pin arrays, triangular pores, etc. The geometry of the stack is expressed in Rott's function *f*. This function is given for some channel geometries in the literature [3]. From Eq.(6.50) one can see that the cooling power is proportional to $I_m(-f_k)$. The real and imaginary parts for some geometry as functions of the ratio the hydraulic radius r_h, which is defined as the ratio of the cross-sectional area and the perimeter of the channel and the thermal penetration depth. The pin arrays and parallel-plates stacks are the best. We note that for parallel-plate stack $r_h = y_0$. The pin-array stack is too difficult to manufacture. Hence, we choose to use a stack made of parallel-plates. The selection of a frequency of 400 Hz, an average pressure of 1bar, and air as working gas, determines the thermal and viscous penetration depths. Using Eq.(5.46) and (5.47) we have δ_k = 0.1mm and δ_v= 0.08 mm. As can be seen from Fig.(7.1) for a parallel-plates stack $I_m(-f_k)$ has a maximum for $r_h/\delta_k = y_0/\delta_k = 1.1$. Since the spacing in the stack is $2y_0$, this means that the optimal spacing is 0.22 mm. But in order not to alter the acoustic field, it was stated to use a spacing of 2δk to 4δk. We choose to use a spacing of about 0.3 mm. The remaining stack geometrical parameters are the center stack position x_s, the length of the stack L_s, and the cross-sectional area A. These parameters are determined from the performance optimization of the stack.

VII.III. Design of the stack

We remain with three stack design parameters: the center position x_n, the length L_{sn} and the cross-sectional area A. By using data for the gas parameters we first optimize the stack geometry parameters by optimizing the performance expressed in terms of the

COP (Eq.(5.8)). This leads to the determination of x_n and L_{sn}. Then the required cooling power will be used to determine the cross-sectional area A. This area is equal to the resonator cross section at the stack location. Once these parameters are determined we can design the resonator. The dissipated acoustic power at the cold side of the resonator forms an extra heat load to the cold heat exchanger. This load, and the required cooling power, will form the total heat load that the cold heat exchanger has to transfer to the stack. The first law of thermodynamics (Eq.(5.6)) states that the total heat load at the hot heat exchanger is the sum of the heat pumped by the stack and the acoustic power used by the stack to realize the heat transfer process. The hot heat exchanger has to remove this heat from the hot side of the stack. The driver has to provide the total needed acoustic power. The design strategy is summarized in Fig.(6.1).

Using the dimensionless parameters, the parameter Γ (Eq.(6.59)) can be rewritten

$$\Gamma = \frac{\Delta T_{mn}}{(\gamma-1)BL_{sn}} \tan(x_n) \tag{7.3}$$

The stack perimeter, Π, can be expressed as function of the cross-sectional area as

$$\Pi = \frac{A}{y_0+l} \tag{7.4}$$

Eqs.(6.56) and (6.55) can be rewritten in a dimensionless form by using the dimensionless parameters, the gas data of Table 7.6, and substitution of Eqs.(6.3) and (6.4),thus

$$Q_{cn} = -\frac{\delta_{kn} D^2 \sin(2x_n)}{8\gamma(1+\sigma)\Lambda}\left(\frac{\Delta T_{mn}\tan(x_n)(1+\sqrt{\sigma}+\sigma)}{BL_{sn}(\gamma-1)(1+\sqrt{\sigma})} - (1+\sqrt{\sigma}-\sqrt{\sigma}\delta_{kn})\right) \tag{7.5}$$

$$W_n = \frac{\delta_{kn} L_{sn} D^2}{4\gamma}(\gamma-1)B\cos(x_n)^2\left(\frac{\Delta T_{mn}\tan(x_n)}{BL_{sn}(\gamma-1)(1+\sqrt{\sigma})\Lambda} - 1\right) - \frac{\delta_{kn} L_{sn} D^2}{4\gamma}\frac{\sqrt{\sigma}\sin(x_n)^2}{B\Lambda} \tag{7.6}$$

$$\Lambda = 1 - \sqrt{\sigma}\delta_{kn} + \frac{1}{2}\sigma\delta_{kn}^2 \tag{7.7}$$

The thermal conductivity term in Eq.(6.56) has been neglected. As discussed earlier, the performance of the stack is expressed in terms of the coefficient of performance

$$COP = \frac{Q_{cn}}{W_n} \tag{7.8}$$

Table 7.6: Parameters used in the performance calculations

Operation parameters	**Gas parameters**
p_m = 1 bar.	a = 346 m/s
T_m = 250 K	σ = 0.68
ΔT_{mn} = 0.3.	γ = 1.67
D = 0.02.	. B = 0.75
f = 400 Hz, k = 2.68 m−1	δ_{kn} = 0.66

VII.IV. OPTIMIZATION OF THE STACK

In the performance calculations, the data shown in Table 7.6 are used. The performance calculations as function of the normalized stack length L_{sn}, for different normalized stack positions x_n. The normalized position x_n = 0, corresponds to the driver position (pressure antinode). In all cases the COP shows a maximum. For each stack length there is an optimal stack position.

As the normalized length of the stack increases, the performance peak shifts to larger stack positions, while the performance decreases. This behavior is to be understood in the following way: A decrease of the center position of the stack means that the stack is placed close to the driver. This position is a pressure antinode and a velocity node, as discussed earlier. Equation (6.55) shows that the viscous losses are proportional to the square of the acoustic velocity. Thus decreasing the velocity will result in a decrease of the losses and hence a higher COP.

In Section V.IV. we discussed the effect of the position of the stack in the standing wave. It was concluded that the maximum cooling power may be expected at a position roughly halfway between the pressure antinode and pressure node (λ/8). The COP peak, the cooling power, and the acoustic power, calculated at the peak position, are plotted as functions of the stack length. The cooling power and the acoustic power increase while the COP decreases as function of the stack length and thus as function of the normalized stack center position. As can be seen from Fig.(7.4),for a normalized stack length above 0.35 the COP is lower than one.

Considering the above remarks and for practical reasons, we have chosen for a normalized stack center position of x_n =0.22. To achieve optimum performance this requires a stack length of L_{sn} = 0.23. Expressed in terms of the normal stack center position and length, we have x_s = 8 cm and Ls = 8.5 cm. This is equivalent to place the hot end of the stack at a distance of 3.75 cm from the driver. Under these conditions the dimensionless cooling power is Q_{cn} = 3.72 .10−6. Since the required cooling power is 4 watt this leads to a cross-sectional area A = 12 cm2. This means a radius of r = 1.9 cm for a cylindrical resonator. To pump 4 watt of heat the stack uses 3 watt of acoustic power (COP = 1.3).

VII.V. RESONATOR

The resonator is designed in order that the length, weight, shape and the losses are optimal. The resonator has to be compact, light, and strong enough. The shape and length are determined by the resonance frequency and minimal losses at the wall of the resonator. The cross-sectional area A of the resonator at the stack location is determined in the preceding Section. As discussed in Section V.III, the resonator can have a λ/2 or a λ/4-length. The viscous and thermal relaxation dissipation losses take place in the penetration depths, along the surface of the resonator. In the boundary-layer approximation, the acoustic power lost per unit surface area of the resonator is given by (Eq.(6.55) with Γ = 0)

$$\frac{d\dot{W}_2}{dS} = \frac{1}{4}\rho_m|\langle u_1\rangle|^2\delta_v\omega + \frac{1}{4}\frac{|p_1|^2}{\rho_m a^2}(\gamma-1)\delta_k\omega \qquad (7.9)$$

where the first term on the right hand side is the kinetic energy dissipated by viscous shear. The second term is the energy dissipated by thermal relaxation. Since the total dissipated energy is proportional to the surface area of the resonator, a λ/4-resonator will dissipate only half the energy dissipated by a λ/2-resonator. Hence a λ/4-resonator is preferable. Hofler shows that the λ/4-resonator can be further optimized by reducing the diameter of the resonator part on the right of the stack. The reason to do this is by minimizing Eq.(7.9). Two parts can be discerned, a large diameter tube (1) containing the stack with diameter D1 and a small diameter tube (2) with diameter D2. The losses in part (2) are plotted as function of the ratio D_1/D_2. The thermal loss increases monotonically as function of the ratio D_1/D_2, but the viscous losses decrease rapidly up to about $D_1/D_2 = 0.5$ and then increase slowly. As a result the total loss (sum) has a minimum at about $D_1/D_2 = 0.54$.

Hoflerand Garrett used a metallic spherical bulb to terminate the resonator. The sphere had sufficient volume to simulate an open end. But at the open end, which is a velocity antinode, the velocity is maximum so that an abrupt transition from the small diameter tube to the bulb can generate turbulence and so losses occur. Taking into account this problem along with the requirement to keep the resonator compact we used a cone-shaped buffer volume to simulate the open end. The calculation optimization of the angle of the cone for minimal losses has been determined to be 90. A gradual tapering is also used between the large diameter tube and small diameter tube. Measurements the standing wave acoustic pressure distribution inside the resonator shows that the system is nearly a quarter-wavelength resonator.

So far we have determined the diameters of the large and small diameter tubes along with the length of the large diameter tube. The total length of the resonator is determined by the desired operation frequency of 400 Hz (k=2.68 m−1). By matching the pressure and volume velocity at the interface between the small and large tube one can deduce the resonance condition which can be used to control the length. The amplitudes of the dynamic pressure and gas velocity due to the standing wave in the large diameter tube (1) are given by

$$p^{(1)} = p_0^{(1)}\cos(kx) \qquad (7.10)$$

And

$$u^{(1)} = \frac{p_0^{(1)}}{\rho_m a}\sin(kx) \qquad (7.11)$$

where the superscript (1) refers to the large diameter tube (1), and $p_0^{(1)}$ is the dynamic pressure amplitude at the driver location (antinode). Pressure and velocity in the small diameter tube (2) are given by

$$p^{(2)} = \frac{p_0^{(2)}}{\rho_m a}\cos(k(L_t - x)) \qquad (7.12)$$

And

$$u^{(2)} = \frac{p_0^{(2)}}{\rho_m a}\cos(k(L_t - x)) \qquad (7.13)$$

where L_t is the total length of the resonator, and subscript (2) refers to the small diameter tube.
At the interface between the two parts at x = l, where l is the length of the large diameter tube (1), the pressure and the volume flow have to be continuous, this can be summarized by saying that the acoustic impedances have to match at the junction.
Thus

$$z^{(1)}(l) = z^{(2)}(l) \qquad (7.14)$$

By substituting

$$z^{(1)}(l) = \frac{p^{(1)}}{A_1 u^{(1)}} = \frac{\cot(kl)}{A_2} \qquad (7.15)$$

and

$$z^{(2)}(l) = \frac{p^{(2)}}{A_1 u^{(2)}} = \frac{\tan(k(L_t - l))}{A_2} \qquad (7.16)$$

Into Eq (6.14), one obtain the resonance condition

$$\cot(kl) = \left(\frac{D1}{D2}\right)^2\tan(k(L_t - l)) \qquad (7.17)$$

where $L_t - l$ is the length of the small diameter tube. Substitution of D_1, D_2, l into Eq.(7.17) yields a total length of L_t = 37.5 cm, so that the length of the small diameter tube is 25 cm. In our calculations we did not take into account the presence of the stack, heat exchangers, tapers, and damping which influence the resonance frequency of the system and hence length.

As discussed earlier, straight tubes have resonance modes which are an integer number of the fundamental mode (ω). We indicated in previous section, that, whenever nonlinear effects exist, higher harmonics may be generated which coincide with the

resonance modes, and hence will be amplified. This means that energy transfer will take place from the fundamental operation mode to the higher oscillation modes. This loss mechanism is to be avoided in thermo acoustic devices. Eq.(7.17) shows that the resonance modes of the resonator having a non uniform cross-section are not an integer number of the fundamental. In this way harmonics can be avoided. Hence, besides the benefit of reducing the losses, the optimized resonator has the advantage of having normal resonance modes which are not an integer number of the fundamental mode. Oberst showed that, using resonators with a shape like can lead to extremely strong standing waves with relatively pure wave forms.

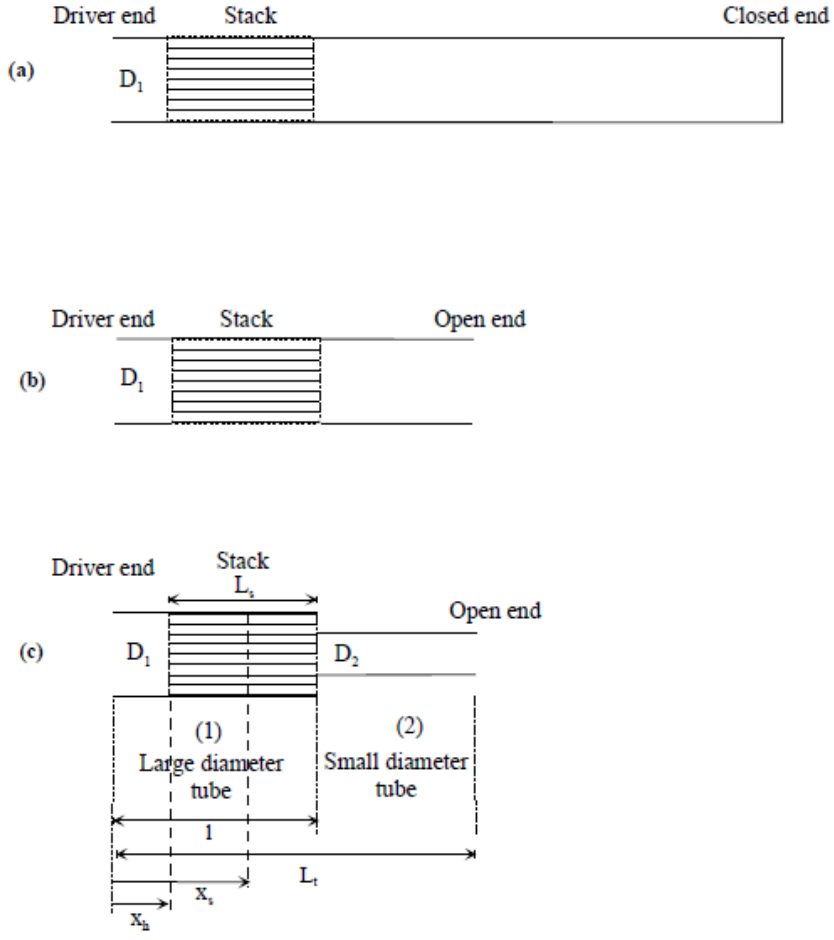

Figure 4.1: Simple resonator design

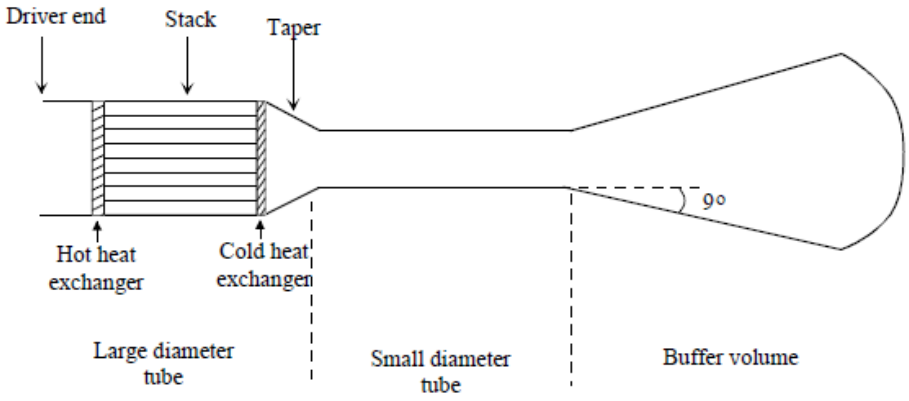

Figure 4.2: Advanced resonator design

The large diameter resonator consists mainly of the stack and the two heat exchangers. Thus, the energy losses take place in these elements. The resonator losses are located at the small diameter tube. The minimal power loss for $D_1/D_2 = 0.54$. These losses are mainly caused by viscous losses. This energy loss shows up as heat at the cold heat exchanger.

VII.VI. HEAT EXCHANGERS

The heat exchangers are necessary to transfer the energy of the thermo acoustic cooling process. The design of the heat exchangers is one of the important problems in thermo acoustics. Little is known about heat transfer in oscillating flows with zero mean velocity. The standard steady-flow design methodology for heat exchangers cannot be applied directly. Furthermore, an understanding of the complex flow patterns at the ends of the stack is also necessary for the design. Nowadays some research groups are using visualization techniques to study these flow patterns which are very complicated. In the following, we will discuss some requirement issues for the design of the heat exchangers.

VII.VI.I. COLD HEAT EXCHANGER

The whole resonator part on the right of the stack cools down so a cold heat exchanger is necessary to make a good thermal contact between the cold side of the stack and the small tube resonator. An electrical heater is placed at the cold heat exchanger to measure cooling power. The length of the heat exchanger is determined by the distance over which heat is transferred by gas. The optimum length corresponds to the peak-to-peak displacement of the gas at the cold heat exchanger location. The displacement amplitude is given by

$$x_1 = \frac{u^{(1)}}{\omega} = \frac{p_0^1}{\omega p_m a}\sin(kx) \qquad (7.18)$$

Substituting the data from Table 7.6, and x = l = 12.5 cm, gives x_1 = 1.47 mm. The optimum length of the cold heat exchanger is thus $2x_1$ = 3 mm. To avoid entrance problems of the gas when leaving the stack and entering the cold heat exchanger or vice versa (continuity of the volume velocity), the porosity of the cold heat exchanger must be equal to the porosity of the stack. This implies that a blockage ratio of 0.75 has to be used in the design of the cold heat exchanger. Acoustic power is also dissipated in the cold heat exchanger. Eq.(6.56) can be used to estimate the dissipated power. Substituting the position of the cold heat exchanger x_n = 0.33, the length L_{hn} =0.008and Γ = 0 (uniform mean temperature)

VII.VI.II. HOT HEAT EXCHANGER

The hot heat exchanger is necessary to remove the heat pumped by the stack and to reject it to the circulating cooling water. As discussed in the precedent subsection, the optimal length of the heat exchanger is equal to the peak-to-peak displacement amplitude of the gas at the heat exchanger location. But since the hot heat exchanger has to reject nearly twice the heat supplied by the cold heat exchanger, the length of the hot heat exchanger should be twice that of the cold heat exchanger (6 mm).Substituting the position of the hot heat exchanger x_n=0.10, the length L_{hn} = 0.016and Γ = 0 into Eq.(6.56)

VII.VII. ACOUSTIC DRIVER

The driver has to provide the total acoustic power used by the stack to transfer heat or dissipated in the different parts. A higher performance of the driver leads to a higher performance of the whole refrigerator system. Furthermore, a high performance of the driver means that the necessary acoustic power can be easily obtained without using high electrical currents which may damage the coil.

VIII. RESULT AND CONCLUSION

Determination of coefficient of performance (C.O.P)

$C.O.P_{REF}=\frac{\text{Heat Generated}}{\text{Work Done}}$

$C.O.P_{REF}=\frac{Q}{W}$

$Q=mC_P\Delta T$

$m=\rho V$

ρ=Refrigerant for air at 1 atm and atmospheric temperature.

Q=Heat extracted.

$V=\left[\frac{\pi}{2}\times d^2\times l\right]+\frac{H}{3}\times[a_1+a_2+\sqrt{a_1a_2}]+1\times 10^{-3}$

$V=[\frac{\pi}{4}\times(20\times10^{-3})^2\times 200\times10^{-3}]+\frac{120\times10^{-3}}{3}\times[\frac{\pi}{4}\times(20\times10^{-3})+\frac{\pi}{4}\times(58\times10^{-3})]+$

$[\sqrt{\frac{\pi}{4}\times(20\times10^{-3})+\frac{\pi}{4}\times(58\times10^{-3})}]$

$V=3.628\times 10^{-3}m^3$

$m=\rho V$

$m=1.2\times 3.628\times 10^{-3}$

$m=4.35\times 10^{-3}\text{kg}/m^3$

$Q=mC_P\Delta T$

$Q=4.35\times 10^{-3}\times 1.005\times 10^{3}\times(5)$

$Q=21.86\ \text{J}$

$C.O.P_{REF}=\frac{Q}{W}$

$C.O.P_{REF}=\frac{21.86}{40}$

$C.O.P_{REF}=0.55$

VIII.I. DESIGNED MODEL

(a): Stack

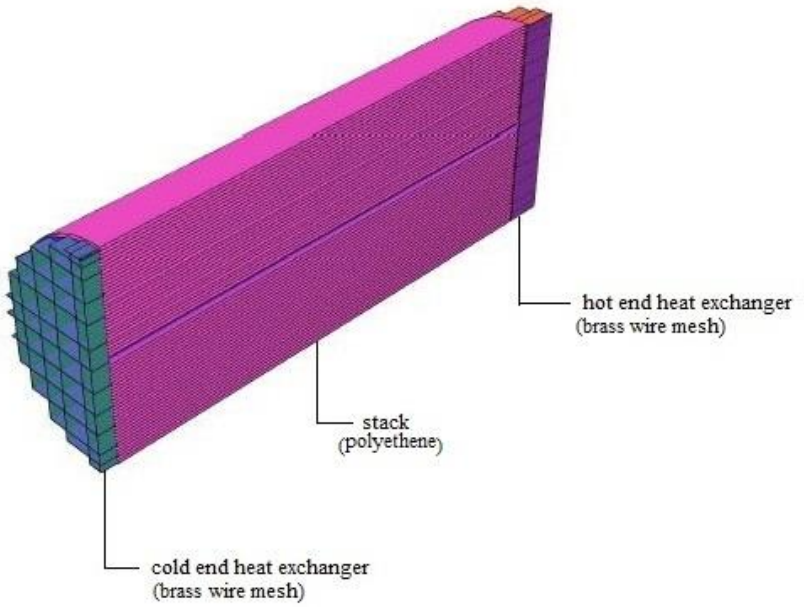

(b): Resonator

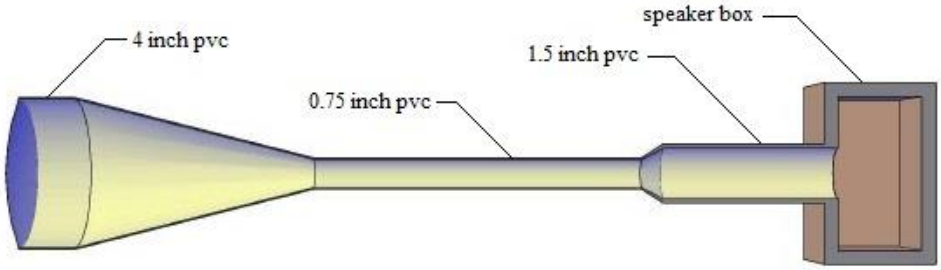

(c): assembled view

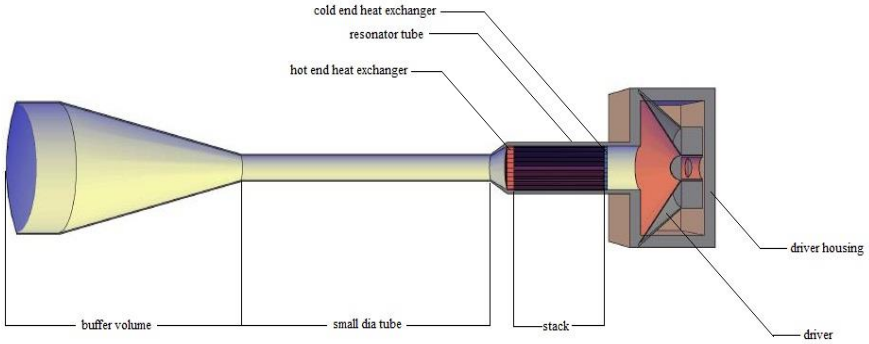

VIII.II. CONCLUSIONS

A thermo acoustic refrigerator is fabricated with readily available materials. The COP of refrigerator is found to be 0.55 it is less efficient when compared with current system. The COP can be improved by replacing working fluid air by some inert gas like helium and also by using pressurized gas instead of using it at the ambient condition.

A few suggestions for the future work include the use of different materials and changing the size and shape of the resonator column. Other possibility is the modification of the stack design and material.

REFERENCES

[1] Lord Rayleigh, .The theory of sound., 2nd edition, Vol.2, Sec.322 (Dover, NewYork, 1995).
[2] N. Rott, .Thermoacoustics., Adv. Appl. Mech. 20, 135 (1990).
[3] K.T. Feldman, Jr., .Review of the literature on Rijke thermoacoustic phenomena., J. Sound Vib. 7, 83 (1988).
[4] N. Rott, .Damped and thermally driven acoustic oscillations in wide and narrowtubes., Z. Angew. Math. Phys. 20, 230 (1989).
[5] G.W. Swift,. Thermoacoustics: A unifying perspective for some enginesand refrigerators., short course, March 1999 Berlin.
[6] G.W. Swift, .Thermoacoustic engines and refrigerators., Encyclopedia of Appliedphysics. 21, 245 (1997).
[7] T.J. Hofler, .Thermoacoustic refrigerator design and performance., Ph.D. dissertation, Physics Department, University of California at San Diego, (1986).
[8] www.navalpostgraduate.com

Authors

First Author – Jinshah B S, Post Graduate student in Energy System Analysis and Design (Mechanical Engineering Department), Government Engineering College, Kozhikode, Kerala, India, E-mail id- jan2live@hotmail.com

Second Author – Ajith Krishnan R, Post graduate student in Energy System Analysis and Design (Mechanical Engineering Department), Government Engineering College, Kozhikode, Kerala, India, E-Mail id- ajithjec@gmail.com

Third Author – Sandeep V S, Post graduate student in Energy System Analysis and Design (Mechanical Engineering Department), Government Engineering College, Kozhikode, Kerala, India E-Mail id- sandualpy@gmail.com